

## ORIGINAL ARTICLE

# The role of brain oscillations in feature integration

M. I. Cobos<sup>1,2</sup>  | M. Melcón<sup>3</sup> | P. Rodríguez-San Esteban<sup>1,2</sup>  | A. Capilla<sup>3</sup>  |  
A. B. Chica<sup>1,2</sup> 

<sup>1</sup>Brain, Mind, and Behavior Research Center (CIMCYC), University of Granada (UGR), Granada, Spain

<sup>2</sup>Department of Experimental Psychology, University of Granada (UGR), Granada, Spain

<sup>3</sup>Department of Biological and Health Psychology, Autonomous University of Madrid (UAM), Madrid, Spain

## Correspondence

M. I. Cobos and A. B. Chica, Department of Experimental Psychology, Faculty of Psychology, University of Granada (UGR), CP: 18071, Granada, Spain.  
Email: [cobosm@ugr.es](mailto:cobosm@ugr.es) and [anachica@ugr.es](mailto:anachica@ugr.es)

## Funding information

FEDER/Ministerio de Ciencia e Innovación - Agencia Estatal de Investigación, Spain, Grant/Award Number: PSI2017-88136 and PID2020-119033 GB-I00 funded by MCIN/AEI/10.13039/501100011033; Spanish Ministry of Economy and Competitiveness, Grant/Award Number: EEBB-PRE2018-084415; Spanish Ministry of Science and Innovation research projects, Grant/Award Number: PSI2017-88136 and PID2020-119033GB-I00; ERDF A way of making Europe, by the European Union; and by FEDER/Junta de Andalucía-Consejería de Economía y Conocimiento/project A.SEI.090. UGR18.

## Abstract

Our sensory system is able to build a unified perception of the world, which although rich, is limited and inaccurate. Sometimes, features from different objects are erroneously combined. At the neural level, the role of the parietal cortex in feature integration is well-known. However, the brain dynamics underlying correct and incorrect feature integration are less clear. To explore the temporal dynamics of feature integration, we studied the modulation of different frequency bands in trials in which feature integration was correct or incorrect. Participants responded to the color of a shape target, surrounded by distractors. A calibration procedure ensured that accuracy was around 70% in each participant. To explore the role of expectancy in feature integration, we introduced an unexpected feature to the target in the last blocks of trials. Results demonstrated the contribution of several frequency bands to feature integration. Alpha and beta power was reduced for hits compared to illusions. Moreover, gamma power was overall larger during the experiment for participants who were aware of the unexpected target presented during the last blocks of trials (as compared to unaware participants). These results demonstrate that feature integration is a complex process that can go wrong at different stages of information processing and is influenced by top-down expectancies.

## KEYWORDS

brain oscillations, errors, expectancy, feature integration

## 1 | INTRODUCTION

At any given moment, our sensory system is overloaded with stimuli that cannot be perceived in isolation. Our

perceptual experience is rich and stimuli need to be integrated into coherent percepts and scenes. Even if our goal is relatively simple (e.g., hit a ball in a tennis match), we cannot only perceive single features such as movement

This is an open access article under the terms of the [Creative Commons Attribution](https://creativecommons.org/licenses/by/4.0/) License, which permits use, distribution and reproduction in any medium, provided the original work is properly cited.

© 2023 The Authors. *Psychophysiology* published by Wiley Periodicals LLC on behalf of Society for Psychophysiological Research.

because other features such as color and shape are important to hit the ball and not another object (a bird passing by). Moreover, humans have the subjective impression of perceiving the whole scene in a very detailed way (in our example, the court, the trees around, the tennis net, etc.). However, this unified perception of large amounts of information has been found to be largely unreliable and full of errors (Block, 2011). Some of these errors consist of incorrect integration of features, for example, erroneously integrating shape and color features from two objects located close to each other (de Gardelle et al., 2009; Humphreys, 2016; Pelli et al., 2004; Pelli & Tillman, 2008; Treisman & Gelade, 1980; Treisman & Schmidt, 1982; Whitney & Levi, 2011).

From a modular conception of the brain, it has been proposed that feature integration is a necessary process because features are processed in different brain regions of the visual hierarchy. Although this problem was partially solved by the discovery of neurons that respond to more than one feature in sensory regions such as V1 (Groen et al., 2017; Shu et al., 2015; Tootell et al., 1998), the computational issue remains unsolved, since additional features may characterize the perceived object.

Behaviorally, errors in feature integration (known as illusory conjunctions) increase when the attentional system is overloaded, in conditions of divided attention (Treisman, 1996; Treisman & Gelade, 1980), when stimuli are briefly presented (Chen & Watanabe, 2021; Henderson & McClelland, 2020; Prinzmetal et al., 1995), when they are presented in the periphery of the visual field (Cohen & Ivry, 1989; Henderson & McClelland, 2020; Prinzmetal et al., 1995; Robertson, 2003; Treisman & Schmidt, 1982), when top-down expectancies are manipulated (Aru et al., 2018; Aru & Bachmann, 2017; Cobos & Chica, 2022; de Gardelle et al., 2009; Kuhn & Rensink, 2016; Mack et al., 2016), and when spatial attention is diverted (Briand, 1998; Cobos & Chica, 2022; Cohen & Rafal, 1991; Grubb et al., 2013; Montaser-Kouhsari & Rajimehr, 2005; Prinzmetal et al., 1986; Yeshurun & Rashal, 2010). Top-down expectancies about perceptual information are well known to bias perception and decision making. Research has demonstrated larger amounts of errors (Engel et al., 2001; Engel & Fries, 2010; Mayer et al., 2016; Min & Herrmann, 2007), including illusory conjunctions, when an unexpected feature appears. Thus, our system tends to complete missing information with the expected perceptual features that we normally encounter in this context.

At the neural level, neuropsychological studies have stressed the role of the parietal cortex in feature integration (Baumgartner et al., 2013; Donner et al., 2000; Esterman et al., 2007; Leonards et al., 2000; Rodríguez-San Esteban et al., 2022; Shafritz et al., 2002); illusory conjunctions increase after damage to this brain area in syndromes such as

hemispatial neglect (Bernstein & Robertson, 1998; Cohen & Rafal, 1991; Cohen-Dallal et al., 2021; Robertson, 2003) or the Balint's syndrome (Chechlacz, 2018; Cohen & Rafal, 1991; Soto & Humphreys, 2009). Brain lesions and functional magnetic resonance imaging (fMRI) data have been important to determine the brain regions supporting correct and incorrect feature integration. Nevertheless, cognitive processing is simultaneously distributed across several spatiotemporal scales, raising the question of how these distinct spectral signatures dynamically interact to enable effective cortical processing and communication (Buzsáki & Draguhn, 2004; Engel et al., 1992, 2001; Fries, 2009; Jensen et al., 2007; Senkowski et al., 2008).

To explore the temporal dynamics of feature integration, we studied the modulation of different frequency bands in trials in which feature integration was correct or incorrect (illusory conjunctions). Previous studies have reported gamma band modulations related to feature integration. For example, gamma activity is higher as the number of features to integrate increases (Honkanen et al., 2015; Keil & Müller, 2010; Morgan et al., 2011; Vidal et al., 2006). This frequency band has been considered a landmark of feature integration (Morgan et al., 2011; Tallon-Baudry, 2009; Tallon-Baudry et al., 1996; Tallon-Baudry & Bertrand, 1999; Vidal et al., 2006), although it has also been related with other cognitive processes such as working memory (Herrmann, Lenz, et al., 2004; Herrmann, Munk, et al., 2004; Miller et al., 2018), selective attention (Gruber et al., 1999; Keil & Müller, 2010; Strüber et al., 2000), and top-down expectancies (Bauer et al., 2014; Rohenkohl et al., 2018). The relation between the beta-band and feature integration is more limited. Beta band modulations are usually associated with motor responses (Engel & Fries, 2010) and top-down signals generated within attentional regions (such as the frontal eye field), which can change the excitability of lower level visual areas (Veniero et al., 2021). Alpha modulations at parieto-occipital electrodes are related to spatial attention (Busch & VanRullen, 2010; Capilla et al., 2014; Kelly et al., 2006; Sauseng et al., 2006; Schroeder et al., 2018; Thut, 2006) and, as outlined above, spatial attention is one of the most important cognitive processes modulating feature integration (Briand, 1998; Cobos & Chica, 2022; Cohen & Rafal, 1991; Grubb et al., 2013; Montaser-Kouhsari & Rajimehr, 2005; Prinzmetal et al., 1986; Yeshurun & Rashal, 2010). In particular, alpha lateralization has been related to spatial selection and inhibition of distractors (Capilla et al., 2014; Klimesch, 2012; Klimesch et al., 2007; Lange et al., 2014; Min & Herrmann, 2007; Schroeder et al., 2018). Conjunction search paradigms have also supported the causal role of alpha oscillations in correct feature integration (Müller et al., 2015). More recently, it has been proposed that alpha/beta power

decreases track the fidelity of stimulus-specific information represented within the cortex (Griffiths et al., 2019). Moreover, early modulations in alpha power (before the stimulation is presented) has been associated to preparatory processes that improve target detection (Ergenoglu et al., 2004; Wutz et al., 2018) and discrimination (Hanslmayr et al., 2007; van den Berg et al., 2016; van Dijk et al., 2008). Finally, there is abundant correlational evidence (Cavanagh et al., 2009; Cohen, 2011; Luu et al., 2004; Trujillo & Allen, 2007) about the role of theta power in error detection, as well as in memory encoding (Roux & Uhlhaas, 2014; Sammer et al., 2007; Sauseng et al., 2010) and false memories (Mapelli & Özkurt, 2019; Sweeney-Reed et al., 2012).

The paradigms used to explore feature integration and illusory conjunctions are diverse, and only one or two frequency bands have been explored in most of the studies addressing the brain dynamics of oscillatory processes associated to correct and incorrect perception (see e.g., Tallon-Baudry & Bertrand, 1999; Zhang et al., 2019). Nevertheless, we posit that different cognitive failures can lead to incorrect feature integration (failures in preparation, spatial attention, or working memory). In order to study the cascade of events that can produce an incorrect feature integration, we used a dual task paradigm (designed to increase the probability of finding erroneous feature integration), titrated to produce ~30% of illusory conjunctions while measuring high-density EEG. Our aim was to compare the spectral signatures of different frequency bands (theta, alpha, beta, and gamma), previously associated to error detection (Cavanagh et al., 2009; Cohen, 2011; Fusco et al., 2018; Luu et al., 2004; Romei et al., 2011; Trujillo & Allen, 2007), preparation (Ergenoglu et al., 2004; Hanslmayr et al., 2007; Mathewson et al., 2009; van den Berg et al., 2016; van Dijk et al., 2008; Wutz et al., 2018), spatial attention (Busch & VanRullen, 2010; Kelly et al., 2006; Sauseng et al., 2006; Schroeder et al., 2018; Thut, 2006), perceptual information representation (Griffiths et al., 2019), top-down influences over visual perception (Veniero et al., 2021), working memory (Herrmann, Lenz, et al., 2004; Herrmann, Munk, et al., 2004; Miller et al., 2018), and feature integration itself (Morgan et al., 2011; Tallon-Baudry, 2009; Tallon-Baudry et al., 1996; Tallon-Baudry & Bertrand, 1999; Vidal et al., 2006). To explore the role of expectancy in feature integration, as done in previous studies (Cobos & Chica, 2022; Rodríguez-San Esteban et al., 2022), we introduced an unexpected feature to the target in the last blocks of trials, and compared brain oscillatory modulations of participants that were aware of this unexpected feature and those that were not aware.

According to the above-reviewed studies, we predicted that incorrect feature integration leading to illusions (as

compared to hits) would be characterized by: (1) an increase in theta power (Cavanagh et al., 2009; Cohen, 2011; Luu et al., 2004; Mapelli & Özkurt, 2019; Roux & Uhlhaas, 2014; Sammer et al., 2007; Sauseng et al., 2010; Sweeney-Reed et al., 2012; Trujillo & Allen, 2007), (2) increased alpha power at early (Ergenoglu et al., 2004; Hanslmayr et al., 2007; van den Berg et al., 2016; van Dijk et al., 2008; Wutz et al., 2018) and late stages, especially at contralateral locations (Busch & VanRullen, 2010; Kelly et al., 2006; Sauseng et al., 2006; Schroeder et al., 2018; Thut, 2006), (3) increased beta power (Griffiths et al., 2019; Veniero et al., 2021), and (4) reduced gamma power (Honkanen et al., 2015; Keil & Müller, 2010; Morgan et al., 2011; Vidal et al., 2006). We had no a-priori hypothesis about the modulations that would be associated to the expectancy manipulation.

## 2 | METHOD

### 2.1 | Participants

G\*power (Faul et al., 2007) was used to calculate the sample size based on the effect size of the proportion of illusions reported in Cobos and Chica (2022; Experiment 3). The effect size in this experiment, reported by rank-biserial correlation ( $r_B$ ), revealed a large effect ( $r_B = -.502$ ;  $d = 1.2$ , Cohen, 1992; Fritz et al., 2012). We calculated sample size for *t*-test Wilcoxon signed-rank test (matched pairs,  $\alpha = 0.05$ ; Power = 0.95). A minimum sample of 12 participants was required. Because we planned to contrast data from aware and unaware participants in the expectancy manipulation (see Method), and because some participants were expected to be excluded from data analyses due to artifacts and noise in the EEG signal, we decided to collect a larger sample of 30 participants.

Thirty healthy volunteers (21 females; mean age of 24 years,  $SD = 2.87$  years) participated in the study in exchange for a monetary compensation of 10€/h. They all reported normal or corrected-to-normal vision, normal color perception, and had no prior experience with the task. Signed informed consent was collected before the study, and participants were informed about their right to withdraw from the experiment at any time. The CEIM/CEI Granada's Biomedicine Ethic Research Committee approved the experiment, which was carried out in accordance with the ethical standards of the 1964 Declaration of Helsinki.

### 2.2 | Stimuli and apparatus

E-Prime software version 2.0 (Schneider et al., 2002) was used to control stimuli presentation, timing operations,

and behavioral data collection. Participants were seated at an approximate distance of 60 cm from the computer screen (an LCD monitor, 24", Benq BL2405HT, 1920×1080 pixels, with a refresh rate of 60 Hz). The experimental procedure was adapted from Esterman and colleagues (Esterman et al., 2004, 2007; see also Cobos & Chica, 2022; Rodríguez-San Esteban et al., 2022).

The display consisted of a central fixation point (a white plus sign,  $0.47^\circ \times 0.47^\circ$ ) presented against a black background. A number was presented above ( $0.95^\circ$ ) the fixation point, printed in white. It could take values between 1 and 9, excluding 5. According to the numerical distance effect (Verguts & Van Opstal, 2005), the numbers conformed two possible conditions: a more demanding "near" condition (numbers closer to 5: 3, 4, 6, 7) and a less demanding "far" condition (numbers further away from 5: 1, 2, 8, 9). The peripheral stimulus consisted of a horizontal string of four characters ( $3.8^\circ \times 1.05^\circ$ ) presented in Arial font. The peripheral stimulus could randomly appear  $5.7^\circ$  to either the right or left side of the fixation point (measured from the center of the fixation point to the inner corner of the string of characters), and  $0.24^\circ$  above the horizontal axis. The two external characters consisted of the flankers "S" or "8", printed in white. The two inner characters were the letters "L" and "O", which were colored in red (RGB: 215,0,0), blue (RGB: 46,118,182), or green (RGB: 0,135,61). In each trial, the "L" and "O" letters always had different colors. Both letters were presented randomly at either the inner leftmost or rightmost location (see Procedure section). A mask (&&&&) was also presented after the string of characters (see Figure 1).

### 2.3 | Procedure

The experiment consisted of 14 blocks of 48 trials, each of them separated by a brief pause. Figure 1 shows the sequence and timing of stimuli in a given trial. Trials began with a fixation screen (with a random duration between 1000 and 2000 ms), followed by the presentation of the number (displayed for a total of 2500 ms). Numbers from the far and the near condition were randomly presented. After 300 ms from the number onset, the peripheral target was shown for 100 ms. Its location was determined randomly, appearing 50% of the trials at each side of the fixation point. After an inter-stimulus interval (ISI) of 50 ms, the mask was displayed for 100 ms.

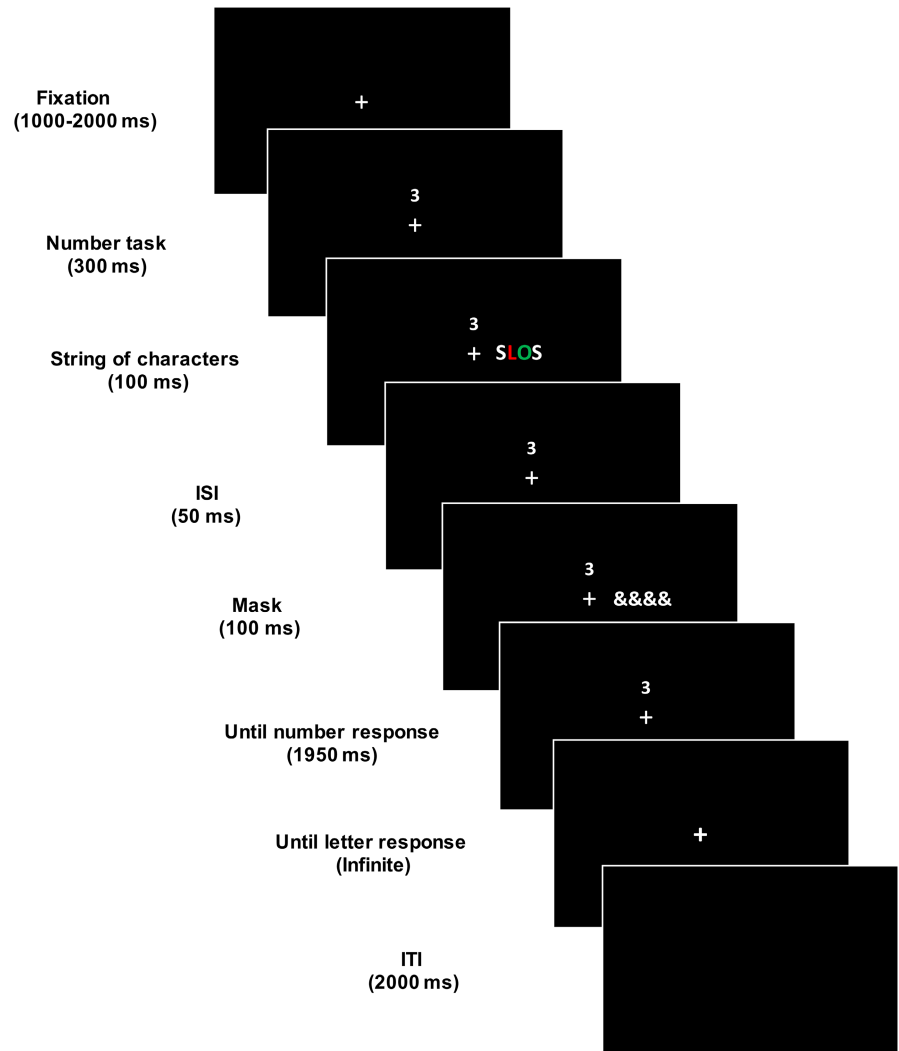
Participants were first required to respond to the number (central task). As soon as the number was presented, they reported whether it was smaller or larger than 5 (using the left or right mouse button, respectively). They used their right hand for this response, performing as fast and accurate as possible.

Once the answer to the central task was given, participants were required to carry out the peripheral task. They were instructed to respond accurately, but without time pressure, using the left hand to press the "z", "x", and "c" keys to report the color of the letter "L" (either red, blue, or green). The correspondence between color and response key was counterbalanced between participants. They could also press the space bar if they were not able to report the color of the target letter. Responses to the peripheral task were categorized as hits (when the correct color of the letter "L" was reported), illusions (when participants reported the color of the letter "O"), errors (when participants reported a color that was not presented in the display), and unseen (when participants could not report the color of the target letter).

Unknown to the participants, in the last four blocks of trials, the target letter was printed in white on 50% of the trials. In these trials, there was no correct response. If participants realized of the presence of the white target, they could report "unseen". They could also respond by saying the color of the distractor (illusion) or a color not presented in the display (error). We will refer to the first 10 blocks as the "expected blocks" and to the last four blocks as the "unexpected blocks". At the end of the experimental session, a brief structured interview was completed to explore whether participants were aware of the appearance of the white letter. Three questions were asked: "Do you have any comments about the experiment?"; "Did you find any color combination more difficult than the others?"; "Have you noticed anything different at the end of the experiment?". After the interview, the objectives of the experiment were explained to the participants, and they were informed about the presence of the white target in the last blocks of trials. At this time, the experimenter confirmed again if participants had perceived the white target or not.

Before the experimental blocks, a separate titration block was presented in order to achieve ~70% hits in each participant. We assumed that the remaining 30% of the trials would be mostly illusions. During titration, trials were similar to the experimental task, except for the size of the string of characters (and the mask). Titration began with the easier condition (size =  $3.8^\circ \times 1.05^\circ$ ; eccentricity from fixation =  $5.7^\circ$ ). After every 14 trials (a titration block), the mean proportion of hits was calculated. If participants correctly reported the color of the peripheral target in 78% or a larger proportion of trials, the size of the string of characters (and the mask) was decreased by  $0.3^\circ \times 0.1^\circ$  for the next titration block. If participants correctly reported the color of the peripheral target in 62% or a fewer proportion of trials, the size of the string of characters (and the mask) was increased by  $0.3^\circ \times 0.1^\circ$  for

**FIGURE 1** Sequence and timing of events in a given trial. Participants first responded to the central task reporting if the number was larger or smaller than 5. After this speeded response was given, participants responded to the peripheral task, indicating the color of the “L” letter with no time pressure.



the next titration block. The titration procedure stopped when the proportion of hits ranged between  $\geq 62\%$  and  $\leq 78\%$  for two consecutive titration blocks. The stimulus size obtained for each participant was used during the experimental trials. The experiment duration (including titration and experimental blocks) was around two and a half hours.

## 2.4 | Behavioral statistical analysis

Behavioral data from the central and the peripheral tasks were analyzed by using non-parametric paired sample *t*-tests (Wilcoxon signed-rank) to compare the mean of proportion of hits, illusions, errors, and unseen responses for the two Central Task conditions (far and near). The effect size is shown by the rank-biserial correlation ( $r_B$ ). If the score is  $< .1$ , it is considered a trivial effect; values around 0.1 are interpreted as small effects, around 0.3 as a medium effect, and  $> 0.5$  as a large effect (Cohen, 1992; Fritz et al., 2012). The Cousineau-Morey's method (Cousineau, 2005; Morey, 2008) was used to

calculate the standard errors of the means represented as error bars.

For the analysis of the central task, accuracy and RT were emphasized. Under these conditions, speed-accuracy trade-off-based strategies can be adopted. That is why we employed the linear integrated speed-accuracy score (LISAS), a measure that combines RT of correct responses (cr) and the proportion of errors (PE) (Vandierendonck, 2017) providing an index of behavioral effects free of these speed-accuracy trade-offs.  $S_{RT}$  refers to the participant's overall RT standard deviation, and  $S_{PE}$  refers to the participant's overall PE standard deviation. Using this index, small values represent faster and/or more accurate responses.

$$LISAS = RT_{cr} + \frac{S_{RT}}{S_{PE}} * PE_{cr}$$

To analyze this index, we run a repeated measures ANOVA with the independent variables of Central Task condition (far and near) and Trial Type (hits and illusions).

To explore the effect of expectancy on feature integration, we performed two analyses. We divided participants into those that were aware of the expectancy manipulation ( $N=14$ ; according to the post-experiment questionnaire) and those that were not aware ( $N=16$ ). Firstly, we compared the proportion of illusions, errors, and unseen trials in the Unexpected blocks (where the peripheral target was printed in white on 50% of the trials; last four blocks of trials) with the trials of the Expected blocks (where the peripheral target was always printed in red, green, or blue; first 10 blocks of trials), introducing Awareness as a between participants' factor in the ANOVA. Secondly, we compared their responses to the Central Task condition (far vs. near) in each Trial Type (hits, illusions, errors, and unseen) during the first 10 blocks of trials. For each group, we subtracted the proportion of responses in each trial type in the far minus the near condition, and compared this index between groups (using a non-parametric independent sample Mann–Whitney test). Since we did not anticipate the number of participants who would be aware of the white target, Bayesian Factor (BF) analysis was applied after recruiting all participants. BF analyses provide conclusive evidence in favor of the alternative ( $BF > 3$ ) or the null hypothesis ( $BF < .33$ ).

## 2.5 | EEG recording

EEG signal was acquired using a 64-channels system mounted on a cap (actiCAP snap, Brain Products) and a computer running the BrainVision Recorder software (version 1.20.0601). Impedances were kept below 5 k $\Omega$ , following the recommendations of the amplifiers' manufacturer, and the signal was digitized at a sampling rate of 1000 Hz. EEG activity was referenced to the FCz electrode online. Electrical activity elicited by horizontal eye movements was monitored by electro-oculogram (EOG), recorded from two electrodes (TP<sub>9</sub>–TP<sub>10</sub>) on the outer canthi of both eyes.

## 2.6 | EEG analysis

While Fieldtrip software (Oostenveld et al., 2011) and in-house built Matlab scripts were used to analyze EEG data, the statistical analysis of these results was performed with JASP (Goss-Sampson, 2019). The general aim of the EEG analyses was to explore how different brain oscillations were related to correct (hits) or incorrect responses (illusions) to the peripheral task, and to the different demands of the central task (near vs. far).

### 2.6.1 | Preprocessing

Data were segmented into 4000 ms long epochs, starting 2000 ms before the number onset. These long epochs were used to avoid undesirable edge effects in the time-frequency (TF) analysis. Only trials in which the participants correctly responded to the central task and provided a response to the peripheral task were used in further analysis.

Five different steps were followed for preprocessing and artifact rejection. (1) The power line artifact at 50 Hz and harmonics (100 and 150 Hz) was reduced via spectrum interpolation (Leske & Dalal, 2019). (2) The baseline was corrected from  $-2000$  to  $0$  ms to facilitate subsequent visualization of EEG traces. (3) All EEG data were visually inspected trial-by-trial and subject-by-subject. Trials which included artifacts such as swallowing, cable movement, or muscular activity were manually rejected. Trials containing blinks or eye-movements 600 ms before or 800 ms after the number onset were also manually rejected. This procedure excluded 11% of the trials ( $SD = 6.5$ ). (4) Independent Component Analysis (“runica” algorithm in Fieldtrip) was used to eliminate any remaining blinks. (5) An average of 2.37 ( $SD = 2.12$ ) channels were interpolated using the signal recorded by neighboring electrodes. Two participants were eliminated because the number of rejected trials exceeded two deviations above the mean. Another participant was discarded because he/she had nine bad channels. Finally, EOG electrodes were removed and EEG data were re-referenced to the common average.

Data were split into different experimental conditions based on the combination of Trial Type (hit or illusion)  $\times$  Peripheral Target Location (left or right).

### 2.6.2 | Time-frequency analysis

Power was calculated for each trial using a (multi-) taper approach (Percival & Walden, 1993). The frequencies analyzed ranged from 2 to 100 Hz in 1 Hz steps. For low frequencies ( $< 30$  Hz), a 400 ms sliding window was applied, while for the gamma frequency ( $> 30$  Hz), we used a 200 ms sliding window. In both cases, the signal was analyzed in 25 ms steps. The resulting TF maps were normalized at the participant level by calculating the relative change from baseline ( $-500$  to  $-200$  ms locked to number onset).

The selection of electrodes and frequency bands is detailed in the supplementary material, Section 1. To avoid the problems of “double dipping” (i.e., the use of the same data for selection and selective analysis Kriegeskorte et al., 2009), we employed the TF representations of

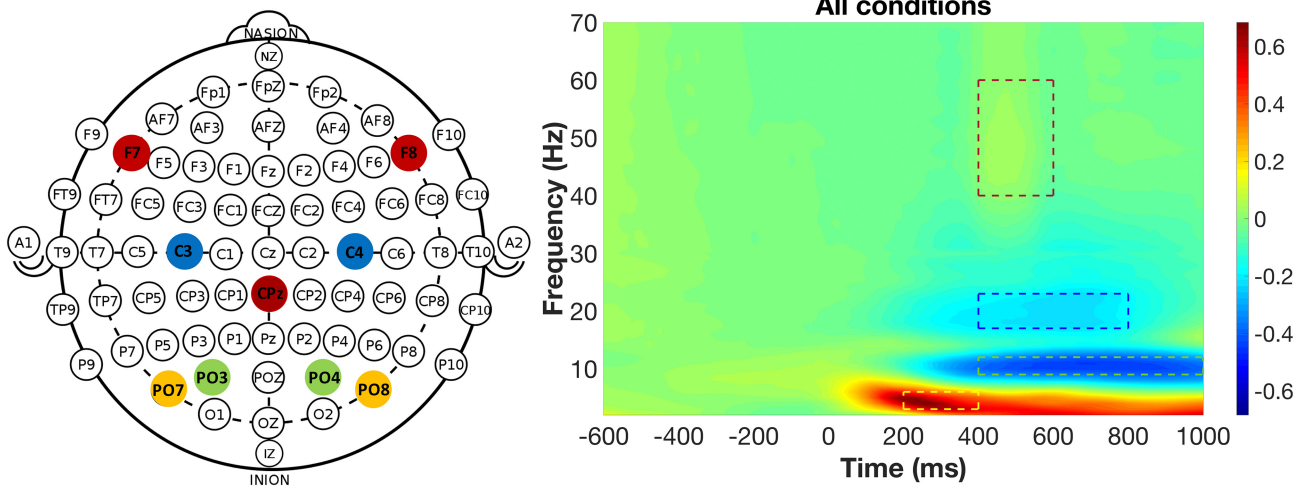


**FIGURE 2** Sketch of the electrodes' distribution around the scalp as viewed from above (the top of the figure represents the frontal area). Additional sites according to the 10–20 International System are shown for further reference. Electrodes selected for analyses of each frequency band are highlighted: PO7-PO8 (yellow circles) for the theta frequency (3–6 Hz); PO3-PO4 (green circles) for the alpha frequency (9–12 Hz); C3-C4 (blue circles) for the beta frequency (17–23 Hz); CPz, F7, and F8 (yellow circles) for the gamma frequency (40–60 Hz). On the right, averaged normalized TF representation (2–70 Hz and –600 to 1000 ms; time 0 ms represents the number onset) for all conditions, participants, and electrodes after bootstrapping. The color bar indicates relative change to baseline (–500 to –200 ms). Dashed lines represent the range of each frequency and the period of time analyzed. The color of the dashed lines corresponds to the color of electrodes.

all conditions pooled together. Thus, we selected the electrodes with the maximum power peak for each frequency band: PO7 and PO8 for theta band (3–6 Hz), PO3 and PO4 for alpha band (9–12 Hz), C3 and C4 for beta band (17–23 Hz) and F7, F8, and CPz for gamma band (30–40 Hz) (Figure 2). FC1 (for the theta band) and CP1 (for the beta band) were also analyzed for showing an additional peak, although the analysis revealed non-significant results in these electrodes (see supplementary material, Section 1.2).

The variables of interest in our paradigm were Central Task condition (far and near) and Trial Type (we focused on hits and illusions for the TF analysis). However, trials were sorted as hits or illusions according to participants' responses, and hits were more likely than illusions (mean of 53.68% hits and 24.74% illusions). The mean number of trials per condition after preprocessing was as follows: Hit-right target: average of 134 ( $\pm 33$ ) trials; Hit-left target: average of 124 ( $\pm 34$ ) trials; Illusion-right target: average of 56 ( $\pm 25$ ) trials, Illusion-left target: average of 63 ( $\pm 31$ ) trials. In order to deal with the effect of this difference in trial number, we used a parametric bootstrapping approach. Firstly, for each participant, we selected the condition with the minimum number of observations (e.g., 30 trials). Then, we randomly selected the same number of trials (30 trials in the example) for each of the other conditions. Secondly, selected trials were averaged leading to a single time series for each condition (Trial Type and Peripheral Target Location) and electrode of interest. This

procedure was repeated 1000 times for each participant resulting in a time  $\times$  1000 matrix per condition and electrode that was finally averaged across the bootstrapping dimension.

Finally, we selected the time windows of interest for each frequency band based on the grand-average of the temporal spectral evolution of all conditions pooled together. Time windows of interest were selected  $\pm 100$  ms from the maximum/minimum peak in each frequency (see supplementary material, Section 1.1 Figures S2, S3, S4, S5).

### 2.6.3 | Statistical analysis of time-frequency maps

Statistical analyses were performed by paired sample *t*-test for peaks observed before the peripheral target was presented (before 300 ms). In these *t*-tests, hits and illusions were compared. Nonetheless, repeated measures analyses of variance (ANOVAs) were applied for peaks observed after the peripheral target was presented (after 300 ms). In these ANOVAs, the variable laterality was also included in the ANOVA. Electrodes were considered ipsilateral or contralateral to the target location: for example, left targets were ipsilateral to the F7 electrode and contralateral to the F8 electrode. When a significant interaction was observed, planned comparisons were conducted using simple main effects in the ANOVA. The variable Central Task was not

introduced in this analysis because it did not behaviorally modulate the proportion of hits and illusions produced by the participants. When only one electrode (i.e., CPz) was statistically tested, paired samples *t*-tests were also applied instead of ANOVAs.

To explore the effect of expectancy on feature integration, we divided participants into those that were aware of the expectancy manipulation ( $N=14$ ; according to the post-experiment questionnaire) and those that were not aware ( $N=16$ ). We compared the overall power in the different frequency bands (theta, alpha, beta and gamma) during the first 10 blocks of trials for participants that were aware and not aware. We did not analyze the results of the last four blocks of trials, because we had not enough trials for this TF analysis.

### 2.6.4 | Post-hoc cross-frequency power–power correlations analysis

Given that some of the observed modulations in the TF analysis were contrary to our hypothesis, we decided to run a post-hoc cross-frequency correlation on a trial-by-trial basis. The range of frequencies (theta: 3–6; alpha: 9–12; beta: 17–23; gamma: 40–60 Hz), electrodes (theta: PO7–PO8; alpha: PO3–PO4; beta: C3–C4; gamma: F7–F8), and time windows selected for the analysis was the same as described above. Trial-by-trial power–power cross-frequency correlations were calculated for each participant and each condition. For each frequency range, random trial selection was performed based on the minimum number of trials among the conditions for each participant. The data were segregated for each channel, allowing for the consolidation of information based on ipsilateral and contralateral data. Note that the CPz electrode in the gamma band was not introduced in this analysis as it was not lateralized. The time period was defined according to the predetermined time window associated with the maximum/minimum peak of each frequency, and the data within that window was averaged. Pearson's correlation scores were calculated between all frequency ranges of interest (early alpha, theta, late alpha, beta, and gamma band) at ipsilateral and contralateral sites. The described procedure was repeated 1000 times, resulting in different sets of randomly selected trials along with corresponding Pearson's correlation scores. The bootstrapped Pearson's correlation scores and the participant's dimensions were averaged. By utilizing the atanh function in Matlab, *Z*-scores were obtained (as done in Bengson et al., 2012; Mazaheri et al., 2009; Mazaheri & Jensen, 2010; Popov et al., 2018), leading to the generation of four different matrices (ipsilateral hits, contralateral hits, ipsilateral illusions, and

contralateral illusions). We first compared if the correlations observed for each condition (hit and illusion) were statistically significant from 0 using a paired sample *t*-test. If one of the correlations (for hits or illusions) in each pair was statistically significant from 0, paired samples *t*-tests were applied to find statistical differences between the *Z*-score in each condition (hits vs. illusions for ipsilateral electrodes and hits vs. illusions for contralateral electrodes; see Figure 11).

## 3 | RESULTS

### 3.1 | Behavioral results

We first analyzed the influence of the Central Task condition in the responses provided to the peripheral task. Neither the proportion of hits ( $W=298$ ,  $p=.184$ ,  $r_B=.282$ ), illusions ( $W=189$ ,  $p=.382$ ,  $r_B=-.187$ ), errors ( $W=219$ ,  $p=.792$ ,  $r_B=-.058$ ), or unseen responses ( $W=36,500$ ,  $p=.552$ ,  $r_B=-.198$ ) were significantly modulated by the Central Task condition (see Figure 3).

We then analyzed RT and accuracy to the central task, as a function of Central task condition (far, near), and categorized the trials as hits or illusions depending on participants' responses to the peripheral task. The analysis of the LISAS index (which combines RT and accuracy, see Methods) demonstrated that responses were more efficient for the “far” as compared to the “near” condition ( $F(1, 28)=65.207$ ,  $MSE=414,409$ ,  $p<.001$ ,  $\eta_p^2=.70$ )<sup>1</sup>. Even though participants had not responded to the peripheral task yet, responses to the central task were more efficient if participants correctly reported the color of the target letter later on the trial (hits) than if an illusion was observed ( $F(1, 28)=22.447$ ,  $MSE=92,579$ ,  $p<.001$ ,  $\eta_p^2=.445$ ) (see Figure 4). The interaction between Central Task and Trial Type was not significant ( $F(1, 28)=2.890$ ,  $MSE=4772$ ,  $p=.100$ ,  $\eta_p^2=.094$ )<sup>1</sup>.

In order to explore whether aware and unaware participants of the presence of the white target during the

<sup>1</sup>RT and accuracy were also analyzed separately (see Section 3, Figures S7 and S8, in the supplementary material, Section 2.2). For RT (in which only trials with correct responses to the central task were analyzed), the ANOVA demonstrated both a main effect of Central Task condition ( $F(1, 28)=88.231$ ,  $MSE=159,975$ ,  $p<.001$ ,  $\eta_p^2=.759$ ), and a main effect of Trial Type ( $F(1, 28)=38.206$ ,  $MSE=43,193$ ,  $p<.001$ ,  $\eta_p^2=.577$ ). The interaction between both variables did not reach significance ( $F(1, 28)=.954$ ,  $MSE=525$ ,  $p=.337$ ,  $\eta_p^2=.033$ ). For the accuracy analysis, a main effect of Central Task ( $F(1, 28)=24.114$ ,  $MSE=.047$ ,  $p<.001$ ,  $\eta_p^2=.463$ ), and a main effect of Trial Type ( $F(1, 28)=5.884$ ,  $MSE=.005$ ,  $p=.022$ ,  $\eta_p^2=.174$ ) were found. The interaction between these factors was not statistically significant ( $F(1, 28)=3.375$ ,  $MSE=.001$ ,  $p=.077$ ,  $\eta_p^2=.108$ ).

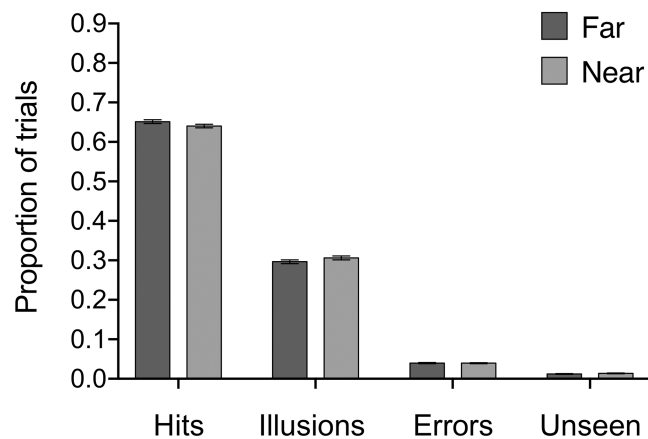


**FIGURE 3** Proportion of hits, illusions, errors, and unseen responses for each Central Task condition (“far” and “near”). This figure shows a comparable number of hits, illusions, errors, and unseen responses in both conditions.

last blocks of trials did already differ in their performance during the expected blocks, Awareness was introduced in the analysis as a between-participants factor. No main effect of Awareness or interactions with this factor were observed (all  $ps > .430$ ).

To explore the role of expectancy on illusory conjunctions, we analyzed the proportion of illusions, errors and responses when the target letter was printed in white in the Unexpected blocks (last four blocks of trials) compared to the Expected blocks (first 10 blocks of trials). Participants who were aware ( $N=14$ ) and not aware ( $N=16$ ) of the expectancy manipulation (presence of the white target in the last block of trials) responded similarly to the task. Both groups made more illusions (not aware:  $W=8$ ,  $p < .001$ ,  $r_B = -.882$ ,  $BF_{10} = 102.807$ ; aware:  $W=3$ ,  $p < .001$ ,  $r_B = -.943$ ,  $BF_{10} = 264.07$ ), errors (not aware:  $W=1$ ,  $p < .001$ ,  $r_B = -.985$ ,  $BF_{10} = 54.97$ ; aware:  $W=8$ ,  $p = .003$ ,  $r_B = -.848$ ,  $BF_{10} = 6.842$ ), and unseen responses (not aware:  $W=1$ ,  $p = .005$ ,  $r_B = -.970$ ,  $BF_{10} = 6.02$ ; aware:  $W=0$ ,  $p = .022$ ,  $r_B = -.848$ ,  $BF_{10} = 4.582$ ), in the Unexpected block compared to Expected block (Figure 5). A direct comparison between both groups (subtracting the proportion of responses in each trial type in the Expected block minus the Unexpected block and comparing this index between groups using a non-parametric independent sample Mann–Whitney  $t$ -tests), indicated that the expectancy effect was comparable for illusions, errors, and unseen responses between groups (all  $ps > .166$ ;  $BF_{10} = 0.678$ ).

Finally, we wondered whether aware and unaware participants responded similarly to the peripheral task during the first 10 blocks of trials (Expected blocks; data represented in Figure 3). A direct comparison between both groups (by subtracting the proportion of responses in far minus near condition), and conducting non-parametric

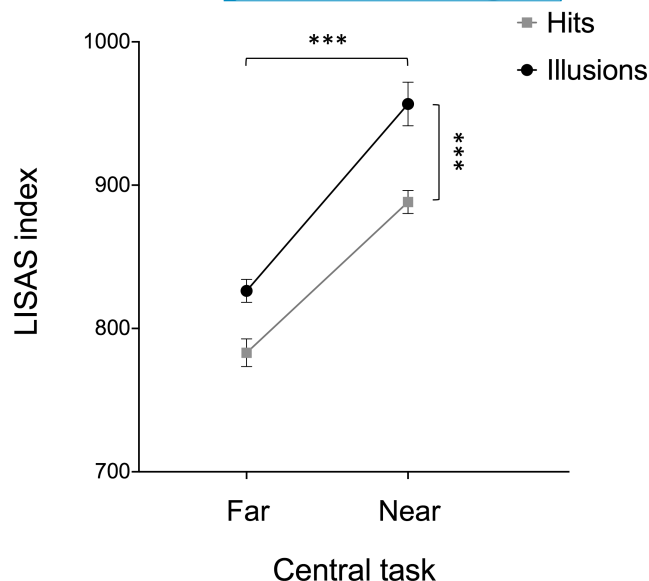


**FIGURE 4** LISAS index to respond to the central task as a function of Central Task condition and Trial Type. This figure shows the main effects of Central Task and Trial Type. Asterisks represent significant effects ( $***p < .001$ ).

independent sample Mann–Whitney  $t$ -tests, revealed that there were no significant differences in the central task effect for illusions, errors, and unseen responses between groups (all  $ps > .093$ ;  $BF_{10} = 1.190$ ).

To sum up, behavioral results show that this paradigm was successful to yield illusory conjunctions (~30% for each participant). A comparable number of illusions were observed for the different Central Task conditions, suggesting that divided attention did not effectively modulate feature integration (Cobos & Chica, 2022; Rodríguez-San Esteban et al., 2022).

Although Central Task demands did not modulate the proportion of illusory conjunctions, we found that participants were slower and less accurate in responding to the central task when, later in the trial, an illusion was reported as compared to hits. Regarding the effect of feature expectancy, the proportion of illusions, errors, and unseen responses significantly increased when the target was unexpectedly presented in white on 50% of the trials (as compared to the Expected block), and this effect was comparable for participants who were aware of the expectancy manipulation and for participants who were not aware.

## 3.2 | Time-frequency results

### 3.2.1 | Power analyses in the peripheral task

The aim of these analyses was to understand the brain oscillatory mechanisms underlying correct versus incorrect feature integration (i.e., hits vs. illusions).

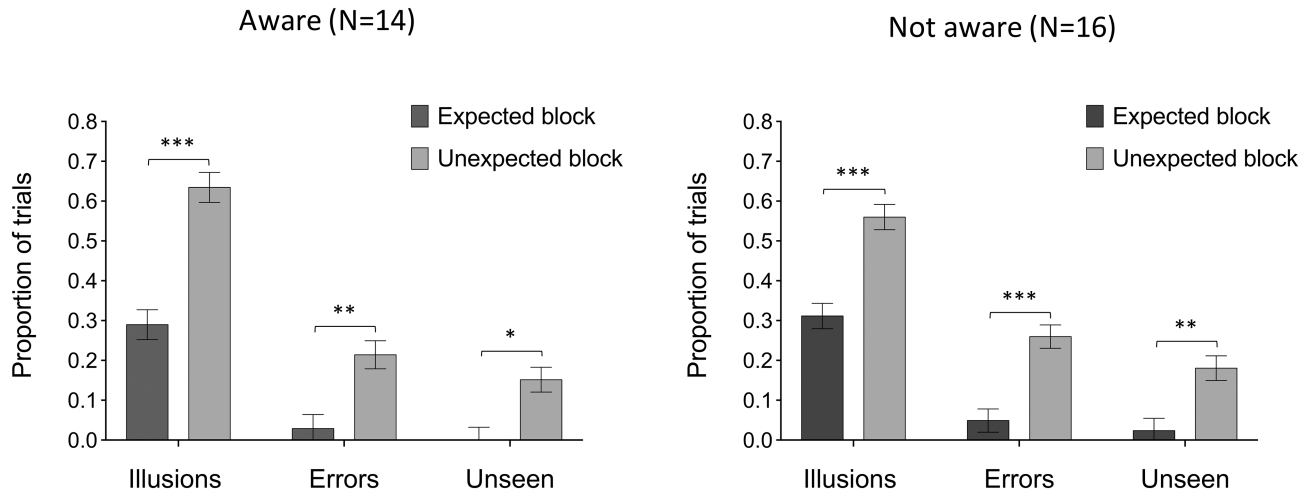


**FIGURE 5** Proportion of illusions, errors, and unseen trials for the Expected blocks and Unexpected blocks. Left panel: aware participants ( $N=14$ ), who noticed that the peripheral target was printed in white in some trials. Right panel: unaware participants ( $N=16$ ), who did not notice that the peripheral target was printed in white in some trials. In the Unexpected block, only trials in which the white target was presented were included in the analysis. Both graphs show the significant increase of illusions, errors, and unseen trials in the Unexpected blocks in comparison with Expected blocks. Asterisks represent statistically significant effects (\*\*\* $p < .001$ ; \*\* $p < .005$ ; \* $p < .05$ ).

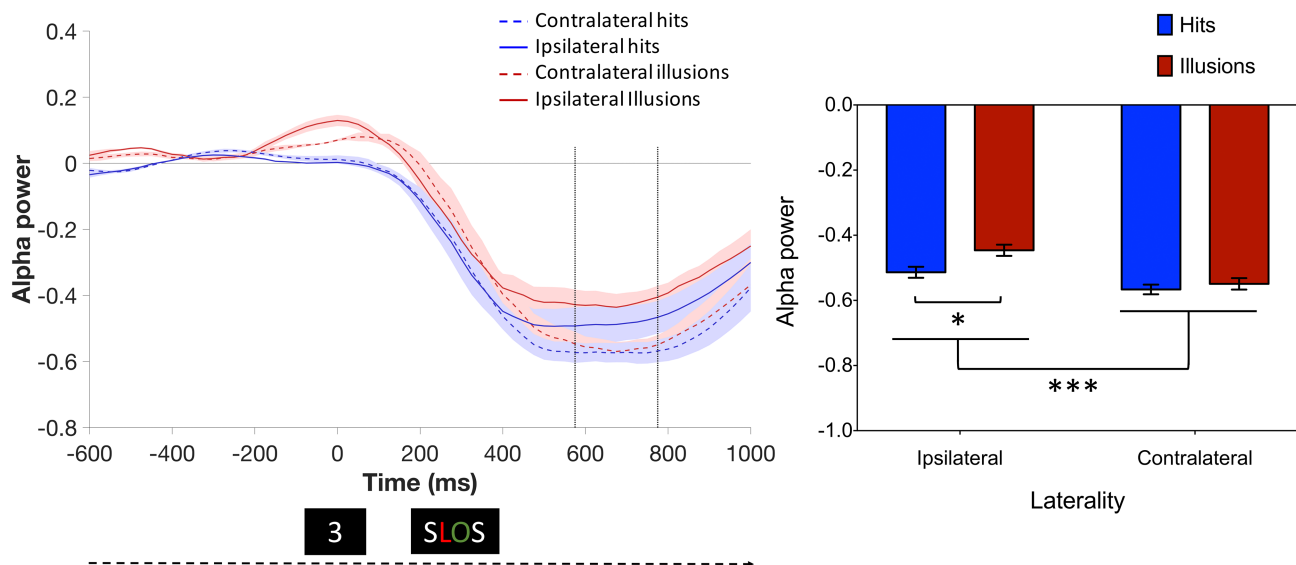


**FIGURE 6** Left panel: Alpha power over time for PO3-PO4 channels averaged. Time 0 represents the onset of the central number. The peripheral target was presented at 300 ms. The vertical dotted lines mark the time interval analyzed (575–775 ms). The shaded area represents the SE of the mean. The right panel represents the main effect of laterality (enhanced alpha suppression for contralateral compared to ipsilateral targets). At ipsilateral electrodes, alpha power showed a greater decrement for hits compared to illusions. Asterisks represent statistically significant effects (\*\*\* $p < .001$ ; \* $p < .05$ ).

Theta power peaked at 200 ms after number onset (100 ms before the peripheral target; see [supplementary material: S2](#)). Theta power from PO7-PO8 electrodes did not differ between hits and illusions ( $t(26) = -0.008$ ,  $p = .994$ , Cohen's  $d = -0.002$ ). Alpha power decreased along the trial, peaking at 675 ms (see [supplementary material: S3](#)). Alpha power decrease was enhanced for contralateral as compared to ipsilateral PO3/PO4 electrodes ( $F(1, 26) = 36.356$ ,  $MSE = 0.005$ ,  $p < .001$ ,  $\eta_p^2 = .583$ ) (see [Figure 6](#)). Interestingly, this Laterality effect interacted

with Trial Type ( $F(1, 26) = 9.819$ ,  $MSE = .002$ ,  $p = .004$ ,  $\eta_p^2 = .274$ ). The planned comparisons showed a greater decrement for hits compared to illusions for ipsilateral electrodes ( $F = 4.686$ ,  $MSE = .062$ ,  $p = .040$ ), while the contralateral electrodes showed no differences ( $F = 0.337$ ,  $MSE = .004$ ,  $p = .566$ ) (see [Figure 6](#)).

As it can be observed in [Figure 6](#), hits and illusions clearly differed in an early time window around time 0. This window (–100 to 100 ms) was analyzed post-hoc, showing a decreased alpha power for hits than illusions

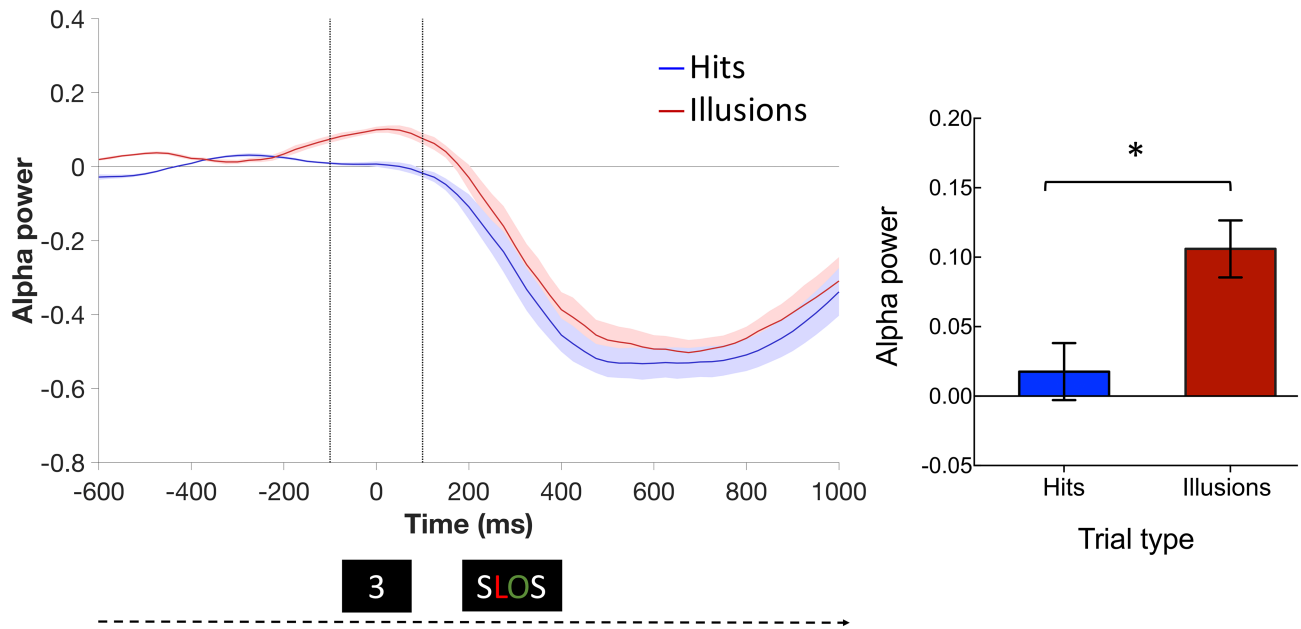


**FIGURE 7** Left panel: Alpha power over time for PO3-PO4 channels averaged. Time 0 represents the onset of the central number. The peripheral target was presented at 300 ms. The vertical dotted lines mark the time interval analyzed (from  $-100$  to  $100$  ms). The shaded area represents the SE of the mean. The right panel represents the main effect of Trial Type. Alpha power was lower for hits compared to illusions. Asterisks represent statistically significant effects ( $*p < .05$ ).

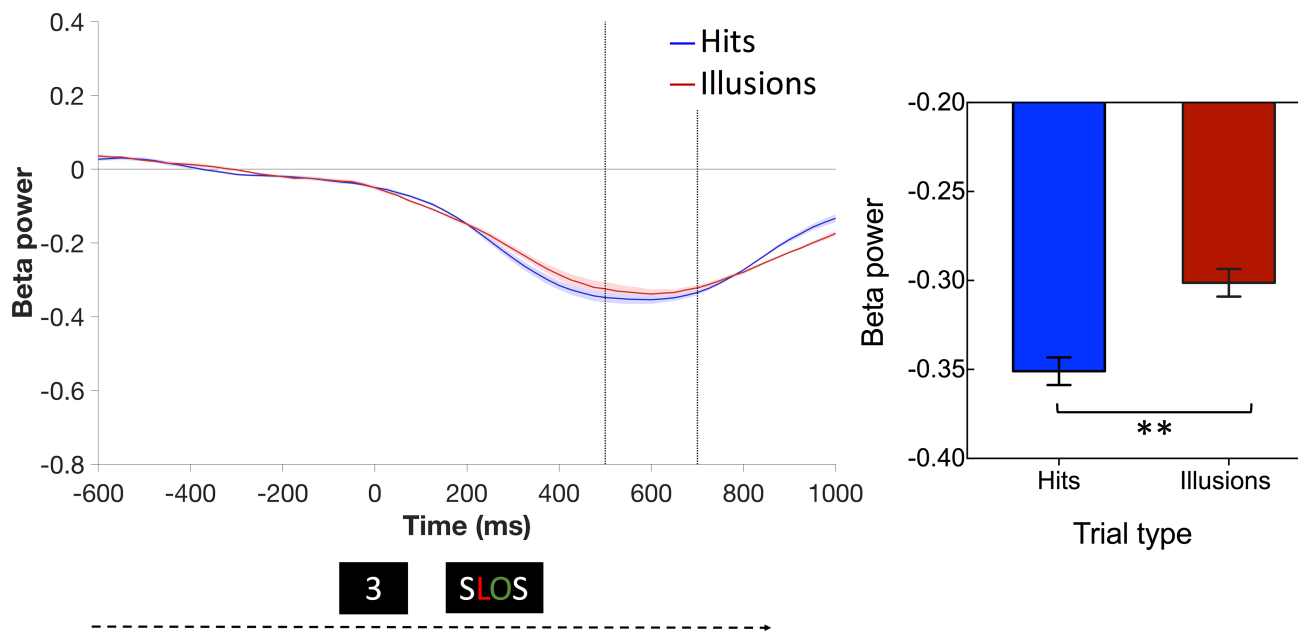


**FIGURE 8** Left panel: Beta power over time for C3-C4 channels averaged. Time 0 represents the onset of the central number. The peripheral target was presented at 300 ms. The vertical dotted lines mark the time interval analyzed ( $500$ – $700$  ms). The shaded area represents the SE of the mean. The right panel represents the main effect of Trial Type. Beta power was more negative for hits compared to illusions. Asterisks represent statistically significant effects ( $**p < .005$ ).

before the peripheral target was presented ( $t(26) = -2.175$ ,  $p = .039$ , Cohen's  $d = -0.419$ , see [Figure 7](#)).

Beta power also decreased after stimuli were presented (peak at  $600$  ms for C3-C4 electrodes; see [supplementary material: S4](#)), and this decrement was enhanced for hits

compared to illusions ( $F(1, 26) = 10.416$ ,  $MSE = .006$ ,  $p = .003$ ,  $\eta_p^2 = .286$ ) (see [Figure 8](#)).

Finally, gamma-band activity (peak at  $450$  ms; see [supplementary material, S5](#)) was larger at frontal locations, and its power was increased for ipsilateral as compared

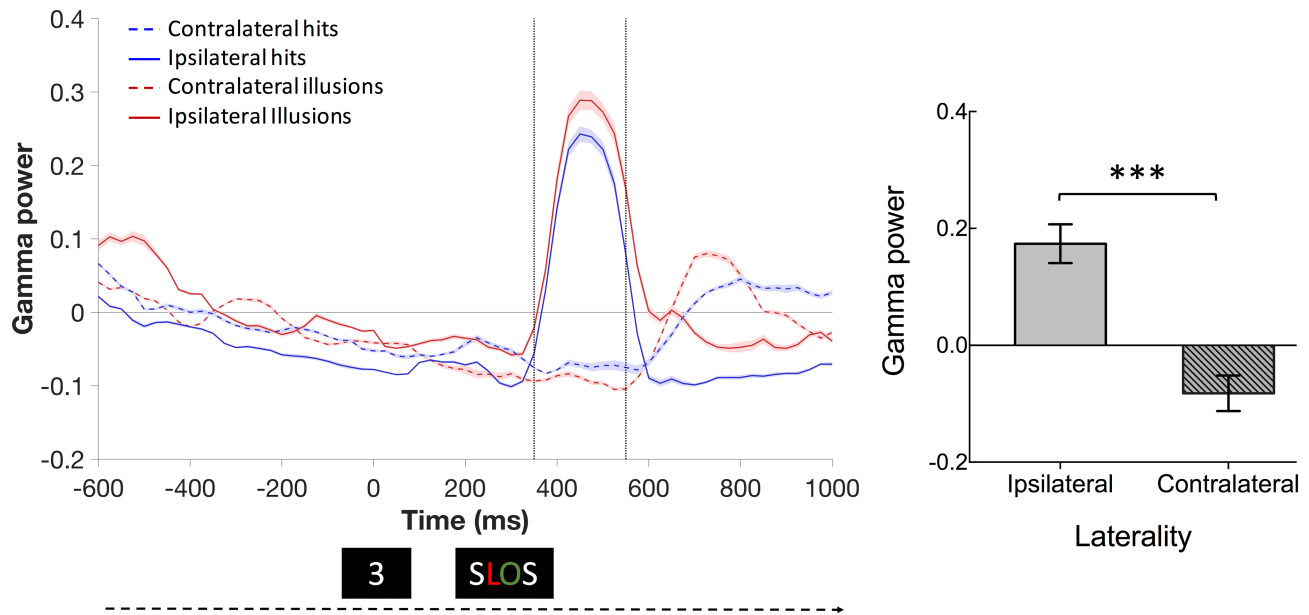


**FIGURE 9** Left panel: Gamma power over time for F7-F8 channels averaged. Time 0 represents the onset of the central number. The peripheral target was presented at 300 ms. The vertical dotted lines mark the time interval analyzed (350–550 ms). The shaded area represents the SE of the mean. The right panel represents the main effect of Laterality: gamma power increased for ipsilateral compared to contralateral target. Asterisks represent statistically significant effects (\*\* $p < .001$ ).

to contralateral electrodes ( $F(1, 26) = 21.008$ ,  $MSE = .084$ ,  $p < .001$ ,  $\eta_p^2 = .447$ ) (see Figure 9). There were no other significant main effects or interactions (all  $F_s < 3.606$ ; all  $p_s > .069$ ).

The behavioral results demonstrated that 16 (out of 30) participants were not aware of the presence of the white target during Unexpected blocks of trials (for EEG analyses only 14 of these participants could be analyzed). We wondered whether aware and unaware participants might have followed a different strategy during the task that could be captured in the TF analyses. To explore this, we repeated the above reported analyses, including the factor Awareness as a between-participants factor. These analyses demonstrated that gamma-band at frontal electrodes was increased for those participants who were aware of the white target as compared to participants who were not aware (main effect of awareness,  $F(1, 25) = 12.817$ ,  $MSE = .101$ ,  $p = .001$ ,  $\eta_p^2 = .339$ ; see Figure 10), especially at ipsilateral electrodes (interaction Laterality  $\times$  Awareness:  $F(1, 25) = 10.983$ ,  $MSE = .061$ ,  $p = .003$ ,  $\eta_p^2 = .305$ ; awareness comparison at ipsilateral electrodes:  $F(1, 25) = 13.166$ ;  $MSE = 1.907$ ;  $p = .001$ ; awareness comparison at contralateral electrodes  $F(1, 25) = 3.052$ ;  $MSE = 0.051$ ;  $p = .093$ ). Gamma power was also increased for those participants who were aware of the white target as compared to participants who were not aware in electrode CPz ( $F(1, 25) = 7.625$ ,  $MSE = .059$ ,  $p = .011$ ,  $\eta_p^2 = .234$ ). There were no other significant main effects or interactions with the factor Awareness (all  $F_s < 12.817$  all  $p_s > .113$ ).

To sum up, these results suggest that errors during feature integration occur at different time intervals and different frequency bands. Illusory conjunctions are associated with oscillations in the alpha and beta bands. Moreover, gamma band activity was also related to the participants' capacity to perceive unexpected features. The implications of these data for feature binding and its relation to attentional processes will be discussed below.

### 3.2.2 | Post-hoc cross-frequency power–power correlation analyses

Given that some of the observed results in the TF analysis were not expected, we decided to perform trial-by-trial cross-frequency power–power correlations. This analysis demonstrated that the correlation between ipsilateral theta and early alpha was larger for illusions than hits ( $Z = 0.143$  vs.  $0.080$ ,  $t(27) = -2.535$ ,  $p = .018$ ). Contralateral early and later alpha showed a larger correlation for illusions than hits ( $Z = 0.092$  vs.  $0.047$ ,  $t(27) = -2.239$ ,  $p = .034$ ). The correlation between contralateral theta and beta power was also larger for illusions than hits ( $Z = 0.043$  vs.  $0.001$ ,  $t(27) = -2.284$ ,  $p = .031$ ) (see Figure 11).

## 4 | DISCUSSION

This study aimed at exploring the role of different brain oscillations in feature integration. The experiment involved

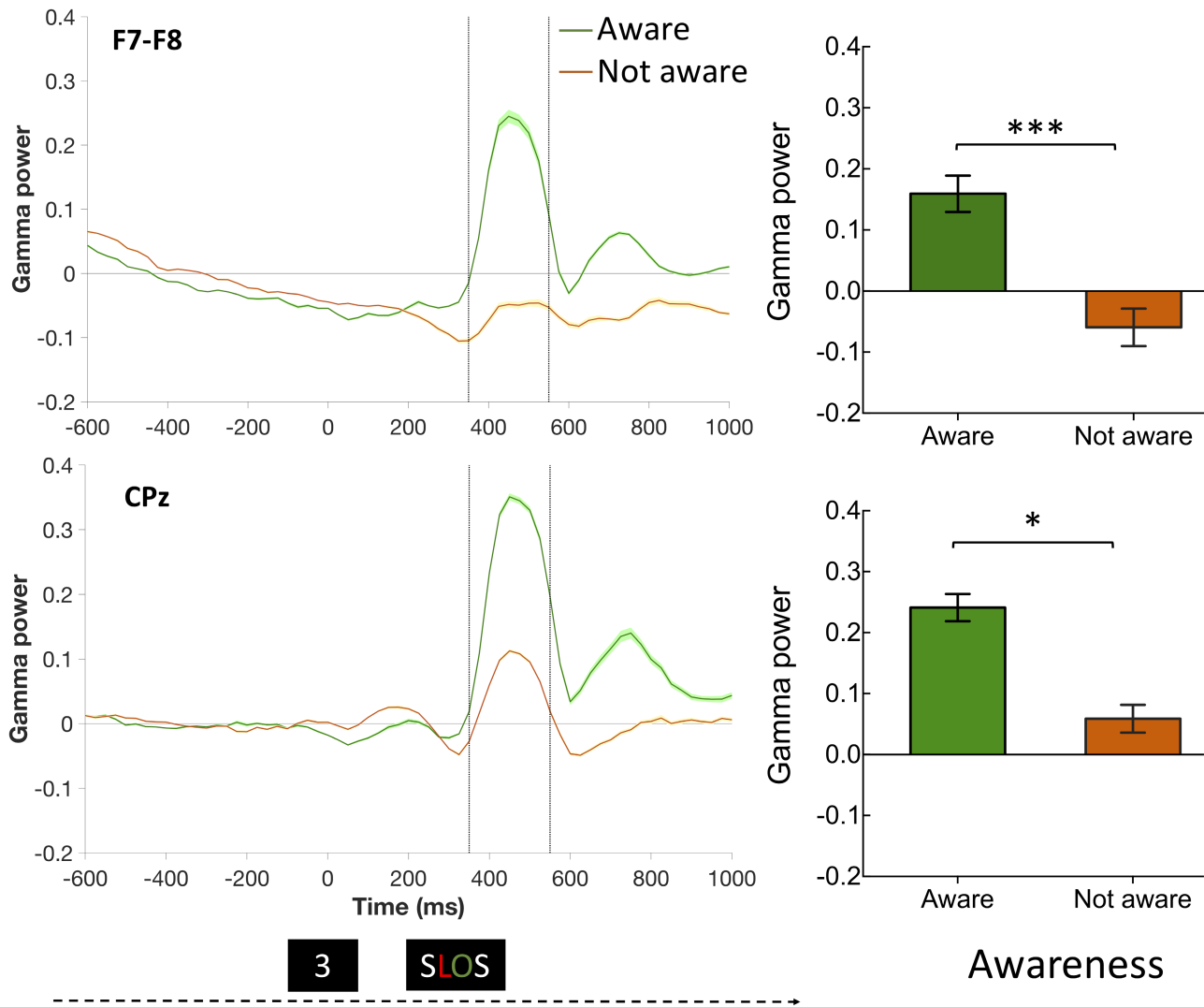


**FIGURE 10** Left panel: Gamma power over time for F7-F8 (averaged) and CPz electrodes. Time 0 represents the onset of the central number. The peripheral target was presented at 300 ms. The vertical dotted lines mark the time interval analyzed (350–550 ms). The shaded area represents the SE of the mean. The right panel represents the main effect Expectancy: gamma power was increased for aware participants compared to not aware participants during the Expected block. Asterisks represent statistically significant effects (\*\* $p < .001$ ; \* $p < .05$ ).

a dual-task combining a central number task (which manipulated attentional demands) and a peripheral task in which color and shape features needed to be integrated (Cobos & Chica, 2022; Esterman et al., 2004, 2007; Rodríguez-San Esteban et al., 2022). Responses were classified as correct (hits, around 70% of the trials) or incorrect (illusions, around 30% of the trials). Behavioral results replicated the observations of previous studies (Cobos & Chica, 2022; Rodríguez-San Esteban et al., 2022): The attentional demands of the number task did not modulate the proportion of trials in which the integration was correct or incorrect. However, responses to the central task were more efficient when feature integration occurred correctly (hits) rather than incorrectly (illusions). This result has been associated with a preparatory process that can occur even before stimuli are presented, and that can

affect performance in both tasks (Cobos & Chica, 2022; Rodríguez-San Esteban et al., 2022) (see also the early alpha modulations discussed below). At the end of the experiment, an unexpected target (a white target) appeared in a proportion of trials. This top-down expectancy manipulation increased illusions, errors, and unseen responses similarly for participants who were aware of the manipulation and for those participants who were not aware of it. It could be argued that the increase in illusions, errors, and unseen trials could be attributed to a decline in sustained attention, indicating fatigue. We analyzed performance across blocks (see supplementary material Section 2.1 and Figure S6) and observed that the proportion of illusions, errors, and unseen trials remained relatively constant during the Expected blocks. Only when non-expected blocks started, we observed a sudden impact on the proportion

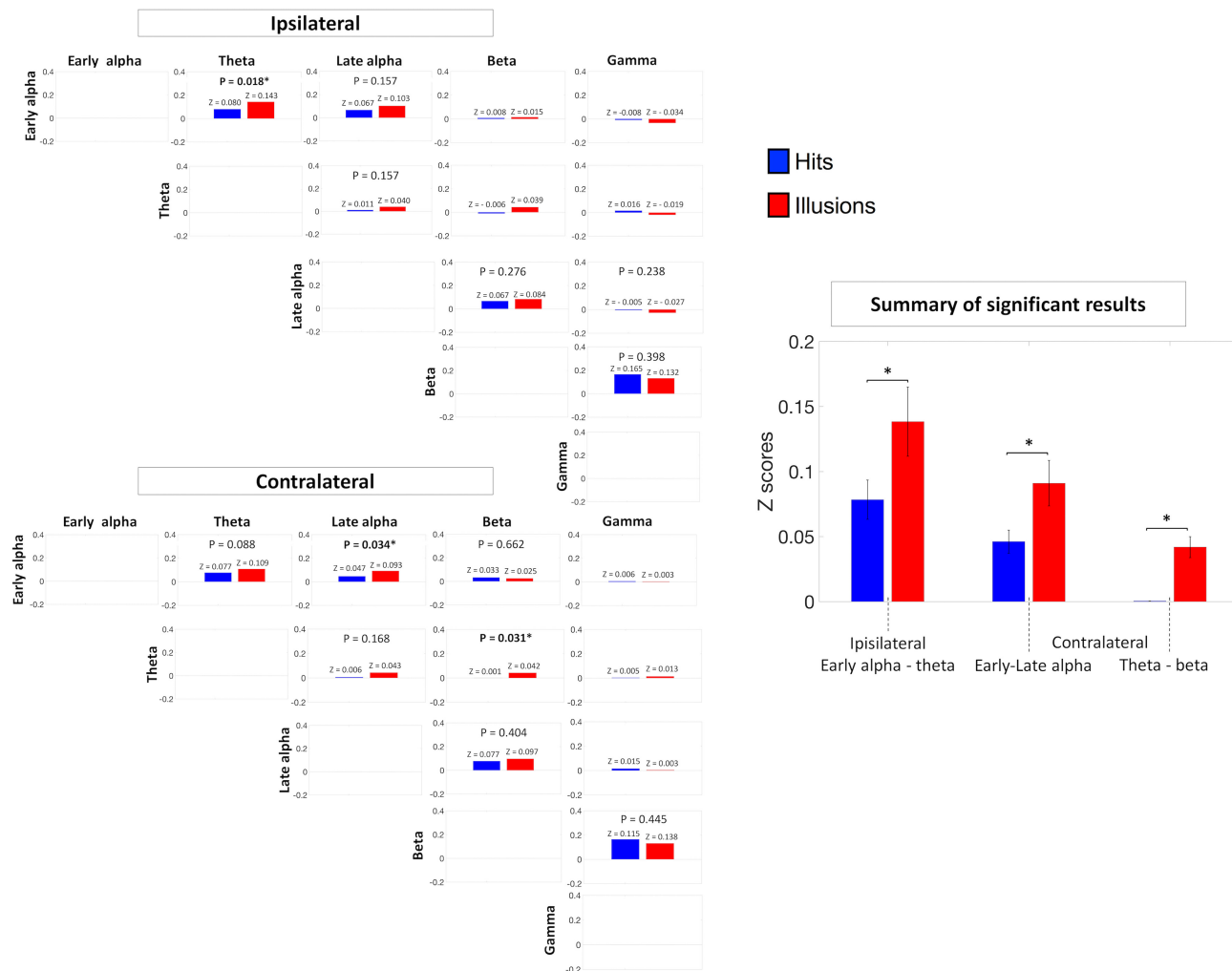


**FIGURE 11** Trial-by-trial Z values correlation for hits versus illusions at ipsilateral and contralateral electrodes. Above the bars, Z and p values are provided. No p values are reported in the comparisons for those pairs in which none of the conditions (hits or illusions) was statistically different from 0. Right panel: summary graph with only the significant correlations ( $*p < .05$ ).

of illusions, errors, and unseen trials. Therefore, we can confidently conclude that the reported behavioral effects of top-down expectations are not influenced by fatigue.

The literature on feature integration is heterogeneous, and generally, only one frequency band is explored. We hypothesized that an incorrect feature integration may be due to failures at different moments and cognitive processes. Thus, in this study, we investigated the contribution of several frequency bands to feature integration and report both early and late modulations. During the early interval (before the peripheral target was presented), alpha power increased for illusions compared to hits. After the peripheral target, alpha and beta power reduction was higher for hits compared to illusions. Finally, a post-hoc trial-by-trial power-power correlation analysis was performed, showing different correlation patterns for correct and incorrect feature integrations.

Previous studies have focused on the gamma band when exploring the brain mechanisms associated with

feature integration (Herrmann, Lenz, et al., 2004; Phillips & Takeda, 2009; Singer, 2013; Tallon-Baudry, 2009). Although there are a large number of experimental paradigms to study errors in feature integration (ambiguous figures, visual search, movement, color, etc.), the gamma band usually increases its power at occipito-parietal electrodes; moreover, gamma power enhancements are more pronounced as task demands for feature integration also increase, and when feature integration is correct rather than incorrect (Bertrand & Tallon-baudry, 2000; Buschman & Miller, 2007; Phillips et al., 2012; Phillips & Takeda, 2009; Vidal et al., 2006). We therefore expected to observe increased gamma power at occipito-parietal electrodes for hits compared to illusions. Instead, gamma power was overall enhanced at frontal electrodes in our results. This apparently contradictory finding might be best accounted for by the literature on working memory, where gamma power increases with increasing memory load (Bastos et al., 2018; Honkanen et al., 2015; Howard, 2003;

Lundqvist et al., 2011; Miller et al., 2018; Roux & Uhlhaas, 2014). Note that our paradigm required maintaining information in working memory, given the brief presentation of stimuli and the use of a dual task. The synaptic attractor model (SAM) states that working memory sample capacity is limited (Awh et al., 2007; Buschman et al., 2011; Cowan, 2010) and the accumulation of elements to be recalled simultaneously causes an amassing of synaptic interference associated with increased gamma activity (Lundqvist et al., 2011; Mi et al., 2017). This suggests that apart from perceptual demands, this task required maintaining information in short-term memory, which might be associated to increases in frontal gamma.

Alpha-band results exhibited early and late modulations. Early modulations (increased alpha for illusions than hits) are in line with the literature showing that alpha power increase is associated with impaired perception (Ergenoglu et al., 2004; Limbach & Corballis, 2016; van Dijk et al., 2008). This result indicates that one of the cognitive processes influencing correct feature integration is the general preparatory state of the organism, which can be related to arousal and activation. In regard to the late alpha modulations observed, it is well-known that alpha power decreases at contralateral as compared to ipsilateral stimulus locations, and this is related to the spatial selection of this location (contralateral modulations) (Busch & VanRullen, 2010; Kelly et al., 2006; Sauseng et al., 2006; Schroeder et al., 2018; Thut, 2006), and the inhibition of distractors (ipsilateral modulations) (Capilla et al., 2014; Klimesch, 2012; Klimesch et al., 2007; Lange et al., 2014; Min et al., 2008; Min & Herrmann, 2007; Schroeder et al., 2018). We expected a larger decrease in contralateral alpha power for hits than illusions. In contrast, we observed an ipsilateral modulation, which might be related to the inhibition of distractors. In general, our data show a larger reduction of alpha and beta power for hits than illusions. Many studies have observed this alpha/beta power reduction in a wide range of cognitive tasks, from visual perception (Pfurtscheller et al., 1996) to memory retrieval (Michelmann et al., 2016). Alpha/beta desynchronization has been associated to information processing in specialized cortical modules during the perception of an event (Jensen & Mazaheri, 2010; Klimesch, 2012). Using representational similarity analysis during the perception and retrieval of videos, Griffiths et al. (2019) have recently demonstrated that alpha/beta power decreases track the fidelity of stimulus-specific information represented within the cortex. This proposal fits well with our data, as alpha and beta power decreases were enhanced for hits compared to illusions, which could be indexing a more reliable representation of perceptual information within the cortex.

Although theta oscillations are strongly associated with perceptual errors (Cavanagh & Frank, 2014;

Cohen, 2011; Fusco et al., 2018; Kalfaoğlu et al., 2018; Mathes et al., 2014), our data showed no modulation in this frequency band. It should be noted that (1) in our data, theta power had its maximal peak before the onset of the peripheral target, and, (2) contrary to previous reports in which frontal theta activity is related to error detection (Cavanagh et al., 2009; Cohen, 2011; Fusco et al., 2018; Luu et al., 2004; Romei et al., 2011; Trujillo & Allen, 2007), theta activity was overall larger at parieto-occipital electrodes in the present study. One possibility is that given the masking and the titration procedure to produce 30% illusions, participants could not distinguish between hits and illusory responses, and therefore, error detection mechanisms were not activated. This possibility will be tested in future studies by introducing a confidence scale after the response.

Given the extensive literature arguing that complex cognitive processes involve communication between different brain oscillations (Fries, 2005, 2009; Rohenkohl et al., 2018), we decided to perform a trial-by-trial power–power correlation between the different frequency bands here explored. We observed an increased correlation for illusions than hits within the alpha band for early and late periods, which indicates that the decrease in alpha power is less pronounced for illusions than for hits throughout the trial. More interestingly, early alpha and theta power correlated positively, and this correlation was increased for illusions as compared to hits. It has been proposed that attention fluctuates in a periodic fashion (Fiebelkorn et al., 2013, 2018; Fiebelkorn & Kastner, 2019; Helfrich et al., 2018), and these fluctuations are associated to performance fluctuations (Busch et al., 2009). For example, Busch and colleagues (Busch et al., 2009; Busch & VanRullen, 2010; van Es et al., 2022) observed that before stimulus onset, alpha and theta phase can account for 16% of variability in detection performance and allow the prediction of performance on the single-trial level (Busch et al., 2009). Our results are in line with these observations, demonstrating that theta and early alpha power are not only associated with stimulus detection but also with the quality of perception; in the current study, increased theta and early alpha power in a given trial is associated with incorrect feature integration.

The theta-beta cross-frequency power–power analysis demonstrated a positive correlation for illusions compared to hits. It means that the correlation implies a higher theta power and a higher decrement in beta power, but other studies indicate the relation between theta and beta using the theta/beta ratio (TBR). The TBR has been applied in different populations (such as Attention-Deficit/Hyperactivity Disorder, ADHD) (Arns et al., 2013; Snyder & Hall, 2006) and in conditions in which attention fluctuated during mind wandering (Son et al., 2019). These

studies have demonstrated an increased theta/beta ratio for ADHD as compared to controls (Arns et al., 2013; Snyder & Hall, 2006), and increased theta/beta ratio during mind wandering (which was related to a decreased connectivity in the executive attention network and increased connectivity in the default mode network (Son et al., 2019; van Son et al., 2019). In the non-clinical population, reduced TBR has also been linked to better cognitive control, executive control, and increased vigilance (Angelidis et al., 2016, 2018; Putman et al., 2010, 2014; van Son et al., 2018). Moreover, TBR may reflect inhibitory cortical and subcortical communications (Knyazev, 2007; Putman et al., 2014; Schutter & Van Honk, 2005), leading by bottom-up and top-down reciprocal systems. In this regard, the TBR may represent the activation of cortical top-down system versus subcortical bottom-up processes (Angelidis et al., 2018; Knyazev, 2007; Putman et al., 2010; Schutter & Van Honk, 2005; van Son et al., 2018). Although the analyses reported in this paper are different from the TBR analysis, the increased correlation of theta-beta observed in illusions as compared to hits could indicate reduced attentional focusing when feature integration failed or bad communication between bottom-up and top-down systems.

In relation to the influence of top-down expectancies in feature integration (Aru et al., 2018; Aru & Bachmann, 2017; Cobos & Chica, 2022; Han & Humphreys, 2007; Humphreys, 2016; Kok et al., 2017), some studies have explored the brain dynamics of different forms of expectancy. Early modulations in alpha power has been related to temporal and multisensorial expectancies (Mayer et al., 2016; Min & Herrmann, 2007). The strength of attentional alpha/beta modulations increases with the predictability of the anticipated sensory target (Bauer et al., 2014; Roehe et al., 2021). Additionally, the presentation of novel stimuli has also been related to increased gamma power (Engel et al., 2001; Engel & Fries, 2010). Our results demonstrate that gamma power was overall larger during the Expected blocks (before the unexpected target presentation) for participants who were aware of the unexpected target presented during the last blocks of trials (as compared to unaware participants). Gamma power increases have been related to attentional selection (Gruber et al., 1999; Herrmann, Lenz, et al., 2004) and to the individual capacity to attend and perceive multiple visual objects concurrently (Rouhinen et al., 2013). Therefore, the difference in gamma power between aware and unaware participants might be due to better attentional selection or capacity to attend to multiple items of the former.

To conclude, our results support that feature integration is a complex process that can go wrong at different stages including attentional processes (early alpha) and perceptual representations (late alpha and beta). They

also highlight the influence of expectations in visual perception, linking gamma-band modulations with the participants' awareness of unexpected events.

## AUTHOR CONTRIBUTIONS

**M. I. Cobos:** Conceptualization; data curation; formal analysis; investigation; methodology; resources; software; supervision; visualization; writing – original draft; writing – review and editing. **M. Melcón:** Formal analysis; methodology; software; writing – review and editing. **P. Rodríguez-San Esteban:** Investigation; resources; writing – review and editing. **A. Capilla:** Formal analysis; methodology; software; writing – review and editing. **A. B. Chica:** Conceptualization; formal analysis; funding acquisition; investigation; methodology; project administration; supervision; writing – original draft; writing – review and editing.

## ACKNOWLEDGMENTS

This paper is part of María I. Cobos doctoral dissertation, which was funded by the PhD grant: EEBB-PRE 2018-084415 (Ministerio de Economía y Competitividad). Ana B. Chica and María Cobos were supported by the Spanish Ministry of Science and Innovation research projects PSI2017-88136 and PID2020-119033GB-I00 and by “ERDF A way of making Europe”, by the “European Union”; and by FEDER/Junta de Andalucía-Consejería de Economía y Conocimiento/project A.SEJ.090. UGR18. Almudena Capilla and María Melcón were supported by FEDER/Ministerio de Ciencia e Innovación—Agencia Estatal de Investigación, Spain (grants PGC2018-100682-B-I00 and PID2021-125841NB-I00).

## DATA AVAILABILITY STATEMENT

All behavioral data analysis and Matlab home-made scripts can be obtained from the open access web: Open Science Framework (OSF). Use the following link to access the information: [https://osf.io/tbwf6/?view\\_only=5efed32f7fb747799cb51952c0917208](https://osf.io/tbwf6/?view_only=5efed32f7fb747799cb51952c0917208). The following software is required to run the data: JASP (Goss-Sampson, 2019), Matlab, and Fieldtrip (Oostenveld et al., 2011).

## ORCID

M. I. Cobos  <https://orcid.org/0000-0002-3856-3189>

P. Rodríguez-San Esteban  <https://orcid.org/0000-0003-2020-9015>

A. Capilla  <https://orcid.org/0000-0002-4181-4284>

A. B. Chica  <https://orcid.org/0000-0001-5804-1591>

## REFERENCES

- Angelidis, A., Hagenaars, M., van Son, D., van der Does, W., & Putman, P. (2018). Do not look away! Spontaneous frontal EEG theta/beta ratio as a marker for cognitive control over

- attention to mild and high threat. *Biological Psychology*, 135, 8–17. <https://doi.org/10.1016/j.biopsycho.2018.03.002>
- Angelidis, A., van der Does, W., Schakel, L., & Putman, P. (2016). Frontal EEG theta/beta ratio as an electrophysiological marker for attentional control and its test-retest reliability. *Biological Psychology*, 121, 49–52. <https://doi.org/10.1016/j.biopsycho.2016.09.008>
- Arns, M., Conners, C. K., & Kraemer, H. C. (2013). A decade of EEG theta/beta ratio research in ADHD: A meta-analysis. *Journal of Attention Disorders*, 17(5), 374–383. <https://doi.org/10.1177/1087054712460087>
- Aru, J., & Bachmann, T. (2017). Expectation creates something out of nothing: The role of attention in iconic memory reconsidered. *Consciousness and Cognition*, 53, 203–210. <https://doi.org/10.1016/j.concog.2017.06.017>
- Aru, J., Tulver, K., & Bachmann, T. (2018). It's all in your head: Expectations create illusory perception in a dual-task setup. *Consciousness and Cognition*, 65, 197–208. <https://doi.org/10.1016/j.concog.2018.09.001>
- Awh, E., Barton, B., & Vogel, E. K. (2007). Visual working memory represents a fixed number of items regardless of complexity. *Psychological Science*, 18(7), 622–628.
- Bastos, A. M., Loonis, R., Kornblith, S., Lundqvist, M., & Miller, E. K. (2018). Laminar recordings in frontal cortex suggest distinct layers for maintenance and control of working memory. *Proceedings of the National Academy of Sciences*, 115(5), 1117–1122. <https://doi.org/10.1073/pnas.1710323115>
- Bauer, M., Stenner, M.-P., Friston, K. J., & Dolan, R. J. (2014). Attentional modulation of alpha/beta and gamma oscillations reflect functionally distinct processes. *Journal of Neuroscience*, 34(48), 16117–16125. <https://doi.org/10.1523/JNEUROSCI.3474-13.2014>
- Baumgartner, F., Hanke, M., Geringswald, F., Zinke, W., Speck, O., & Pollmann, S. (2013). Evidence for feature binding in the superior parietal lobule. *NeuroImage*, 68, 173–180. <https://doi.org/10.1016/j.neuroimage.2012.12.002>
- Bengson, J. J., Mangun, G. R., & Mazaheri, A. (2012). The neural markers of an imminent failure of response inhibition. *NeuroImage*, 59(2), 1534–1539. <https://doi.org/10.1016/j.neuroimage.2011.08.034>
- Bernstein, L. J., & Robertson, L. C. (1998). Illusory conjunctions of color and motion with shape following bilateral parietal lesions. *Psychological Science*, 9(3), 167–175. <https://www.jstor.org/stable/40063274>
- Bertrand, O., & Tallon-Baudry, C. (2000). Oscillatory gamma activity in humans: A possible role for object representation. *International Journal of Psychophysiology*, 38(3), 211–223. [https://doi.org/10.1016/S0167-8760\(00\)00166-5](https://doi.org/10.1016/S0167-8760(00)00166-5)
- Block, N. (2011). Perceptual consciousness overflows cognitive access. *Trends in Cognitive Sciences*, 15(12), 567–575. <https://doi.org/10.1016/j.tics.2011.11.001>
- Briand, K. A. (1998). Feature integration and spatial attention: More evidence of a dissociation between endogenous and exogenous orienting. *Journal of Experimental Psychology: Human Perception and Performance*, 24(4), 1243–1256. <https://doi.org/10.1037/0096-1523.24.4.1243>
- Busch, N. A., Dubois, J., & VanRullen, R. (2009). The phase of ongoing EEG oscillations predicts visual perception. *Journal of Neuroscience*, 29(24), 7869–7876. <https://doi.org/10.1523/JNEUROSCI.0113-09.2009>
- Busch, N. A., & VanRullen, R. (2010). Spontaneous EEG oscillations reveal periodic sampling of visual attention. *Proceedings of the National Academy of Sciences*, 107(37), 16048–16053. <https://doi.org/10.1073/pnas.1004801107>
- Buschman, T. J., & Miller, E. K. (2007). Top-down versus bottom-up control of attention in the prefrontal and posterior parietal cortices. *Science*, 315(5820), 1860–1862. <https://doi.org/10.1126/science.1138071>
- Buschman, T. J., Siegel, M., Roy, J. E., & Miller, E. K. (2011). Neural substrates of cognitive capacity limitations. *Proceedings of the National Academy of Sciences*, 108(27), 11252–11255. <https://doi.org/10.1073/pnas.1104666108>
- Buzsáki, G., & Draguhn, A. (2004). Neuronal oscillations in cortical networks. *Science*, 304(5679), 1926–1929. <https://doi.org/10.1126/science.1099745>
- Capilla, A., Schoffelen, J.-M., Paterson, G., Thut, G., & Gross, J. (2014). Dissociated  $\alpha$ -band modulations in the dorsal and ventral visual pathways in visuospatial attention and perception. *Cerebral Cortex (New York, NY)*, 24(2), 550–561. <https://doi.org/10.1093/cercor/bhs343>
- Cavanagh, J., Cohen, M., & Allen, J. (2009). Prelude to and resolution of an error: EEG phase synchrony reveals cognitive control dynamics during action monitoring. *The Journal of Neuroscience*, 29, 98–105. <https://doi.org/10.1523/JNEUROSCI.4137-08.2009>
- Cavanagh, J. F., & Frank, M. J. (2014). Frontal theta as a mechanism for cognitive control. *Trends in Cognitive Sciences*, 18(8), 414–421. <https://doi.org/10.1016/j.tics.2014.04.012>
- Chechlacz, M. (2018). Bilateral parietal dysfunctions and disconnections in simultanagnosia and Bálint syndrome. *Handbook of Clinical Neurology*, 151, 249–267. <https://doi.org/10.1016/B978-0-444-63622-5.00012-7>
- Chen, N., & Watanabe, K. (2021). Color–shape associations affect feature binding. *Psychonomic Bulletin & Review*, 28(1), 169–177. <https://doi.org/10.3758/s13423-020-01799-4>
- Cobos, M. I., & Chica, A. B. (2022). Attention does not always help: The role of expectancy, divided, and spatial attention on illusory conjunctions. *Quarterly Journal of Experimental Psychology*, 75, 2087–2104. <https://doi.org/10.1177/17470218221089625>
- Cohen, A., & Ivry, R. (1989). Illusory conjunctions inside and outside the focus of attention. *Journal of Experimental Psychology: Human Perception and Performance*, 15(4), 650–663. <https://doi.org/10.1037/0096-1523.15.4.650>
- Cohen, A., & Rafal, R. D. (1991). Attention and feature integration: Illusory conjunctions in a patient with a parietal lobe lesion. *Psychological Science*, 2(2), 106–110. <https://doi.org/10.1111/j.1467-9280.1991.tb00109.x>
- Cohen, J. (1992). A power primer. *Psychological Bulletin*, 112(1), 155–159. <https://doi.org/10.1037/0033-2909.112.1.155>
- Cohen, M. X. (2011). Error-related medial frontal theta activity predicts cingulate-related structural connectivity. *NeuroImage*, 55(3), 1373–1383. <https://doi.org/10.1016/j.neuroimage.2010.12.072>
- Cohen-Dallal, H., Soroker, N., & Pertzov, Y. (2021). Working memory in unilateral spatial neglect: Evidence for impaired binding of object identity and object location. *Journal of Cognitive Neuroscience*, 33(1), 46–62. [https://doi.org/10.1162/jocn\\_a\\_01631](https://doi.org/10.1162/jocn_a_01631)



- Cousineau, D. (2005). Confidence intervals in within-subject designs: A simpler solution to Loftus and Masson's method. *Tutorials in Quantitative Methods for Psychology*, *1*(1), 42–45. <https://doi.org/10.20982/tqmp.01.1.p042>
- Cowan, N. (2010). The magical mystery four: How is working memory capacity limited, and why? *Current Directions in Psychological Science*, *19*(1), 51–57. <https://doi.org/10.1177/0963721409359277>
- de Gardelle, V., Sackur, J., & Kouider, S. (2009). Perceptual illusions in brief visual presentations. *Consciousness and Cognition*, *18*(3), 569–577. <https://doi.org/10.1016/j.concog.2009.03.002>
- Donner, T., Kettermann, A., Diesch, E., Ostendorf, F., Villringer, A., & Brandt, S. A. (2000). Involvement of the human frontal eye field and multiple parietal areas in covert visual selection during conjunction search. *European Journal of Neuroscience*, *8*, 3407–3414.
- Engel, A. K., & Fries, P. (2010). Beta-band oscillations—Signalling the status quo? *Current Opinion in Neurobiology*, *20*(2), 156–165. <https://doi.org/10.1016/j.conb.2010.02.015>
- Engel, A. K., Fries, P., & Singer, W. (2001). Dynamic predictions: Oscillations and synchrony in top-down processing. *Nature Reviews Neuroscience*, *2*(10), 704–716. <https://doi.org/10.1038/35094565>
- Engel, A. K., König, P., Kreiter, A. K., Schillen, T. B., & Singer, W. (1992). Temporal coding in the visual cortex: New vistas on integration in the nervous system. *Trends in Neurosciences*, *15*(6), 218–226. [https://doi.org/10.1016/0166-2236\(92\)90039-B](https://doi.org/10.1016/0166-2236(92)90039-B)
- Ergenoglu, T., Demiralp, T., Bayraktaroglu, Z., Ergen, M., Beydagi, H., & Uresin, Y. (2004). Alpha rhythm of the EEG modulates visual detection performance in humans. *Cognitive Brain Research*, *20*(3), 376–383. <https://doi.org/10.1016/j.cogbrainres.2004.03.009>
- Esterman, M., Prinzmetal, W., & Robertson, L. (2004). Categorization influences illusory conjunctions. *Psychonomic Bulletin & Review*, *11*(4), 681–686. <https://doi.org/10.3758/BF03196620>
- Esterman, M., Verstynen, T., & Robertson, L. C. (2007). Attenuating illusory binding with TMS of the right parietal cortex. *NeuroImage*, *35*(3), 1247–1255. <https://doi.org/10.1016/j.neuroimage.2006.10.039>
- Faul, F., Erdfelder, E., Lang, A.-G., & Buchner, A. (2007). G\*Power 3: A flexible statistical power analysis program for the social, behavioral, and biomedical sciences. *Behavior Research Methods*, *39*(2), 175–191. <https://doi.org/10.3758/BF03193146>
- Fiebelkorn, I. C., & Kastner, S. (2019). A rhythmic theory of attention. *Trends in Cognitive Sciences*, *23*(2), 87–101. <https://doi.org/10.1016/j.tics.2018.11.009>
- Fiebelkorn, I. C., Pinsk, M. A., & Kastner, S. (2018). A dynamic interplay within the frontoparietal network underlies rhythmic spatial attention. *Neuron*, *99*(4), 842–853.e8. <https://doi.org/10.1016/j.neuron.2018.07.038>
- Fiebelkorn, I. C., Saalman, Y. B., & Kastner, S. (2013). Rhythmic sampling within and between objects despite sustained attention at a cued location. *Current Biology*, *23*(24), 2553–2558. <https://doi.org/10.1016/j.cub.2013.10.063>
- Fries, P. (2005). A mechanism for cognitive dynamics: Neuronal communication through neuronal coherence. *Trends in Cognitive Sciences*, *9*(10), 474–480. <https://doi.org/10.1016/j.tics.2005.08.011>
- Fries, P. (2009). Neuronal gamma-band synchronization as a fundamental process in cortical computation. *Annual Review of Neuroscience*, *32*(1), 209–224. <https://doi.org/10.1146/annurev-neuro.051508.135603>
- Fritz, C. O., Morris, P. E., & Richler, J. J. (2012). Effect size estimates: Current use, calculations, and interpretation. *Journal of Experimental Psychology: General*, *141*(1), 2–18. <https://doi.org/10.1037/a0024338>
- Fusco, G., Scandola, M., Feurra, M., Pavone, E. F., Rossi, S., & Aglioti, S. M. (2018). Midfrontal theta transcranial alternating current stimulation modulates behavioural adjustment after error execution. *European Journal of Neuroscience*, *48*(10), 3159–3170. <https://doi.org/10.1111/ejn.14174>
- Goss-Sampson, M. (2019). *Statistical analysis in JASP: A guide for students*. JASP. <https://jasp-stats.org/jasp-materials/>
- Griffiths, B. J., Mayhew, S. D., Mullinger, K. J., Jorge, J., Charest, I., Wimber, M., & Hanslmayr, S. (2019). Alpha/beta power decreases track the fidelity of stimulus-specific information. *eLife*, *8*, e49562. <https://doi.org/10.7554/eLife.49562>
- Groen, I. I., Silson, E. H., & Baker, C. I. (2017). Contributions of low- and high-level properties to neural processing of visual scenes in the human brain. *Philosophical Transactions of the Royal Society B: Biological Sciences*, *372*(1714), 20160102. <https://doi.org/10.1098/rstb.2016.0102>
- Grubb, M. A., Behrmann, M., Egan, R., Minshew, N. J., Heeger, D. J., & Carrasco, M. (2013). Exogenous spatial attention: Evidence for intact functioning in adults with autism spectrum disorder. *Journal of Vision*, *13*(14), 9. <https://doi.org/10.1167/13.14.9>
- Gruber, T., Müller, M. M., Keil, A., & Elbert, T. (1999). Selective visual-spatial attention alters induced gamma band responses in the human EEG. *Clinical Neurophysiology*, *110*(12), 2074–2085. [https://doi.org/10.1016/S1388-2457\(99\)00176-5](https://doi.org/10.1016/S1388-2457(99)00176-5)
- Han, S., & Humphreys, G. W. (2007). The fronto-parietal network and top-down modulation of perceptual grouping. *Neurocase*, *13*(4), 278–289. <https://doi.org/10.1080/13554790701649930>
- Hanslmayr, S., Aslan, A., Staudigl, T., Klimesch, W., Herrmann, C. S., & Bäuml, K.-H. (2007). Prestimulus oscillations predict visual perception performance between and within subjects. *NeuroImage*, *37*(4), 1465–1473. <https://doi.org/10.1016/j.neuroimage.2007.07.011>
- Helfrich, R. F., Fiebelkorn, I. C., Szczepanski, S. M., Lin, J. J., Parvizi, J., Knight, R. T., & Kastner, S. (2018). Neural mechanisms of sustained attention are rhythmic. *Neuron*, *99*(4), 854–865.e5. <https://doi.org/10.1016/j.neuron.2018.07.032>
- Henderson, C. M., & McClelland, J. L. (2020). Intrusions into the shadow of attention: A new take on illusory conjunctions. *Attention, Perception, & Psychophysics*, *82*, 564–584. <https://doi.org/10.3758/s13414-019-01893-3>
- Herrmann, C. S., Lenz, D., Junge, S., Buch, N. A., & Maess, B. (2004). Memory-matches evoke human gamma-responses. *BMC Neuroscience*, *5*(13), 1–8. <https://doi.org/10.1186/1471-2202-5-13>
- Herrmann, C. S., Munk, M. H. J., & Engel, A. K. (2004). Cognitive functions of gamma-band activity: Memory match and utilization. *Trends in Cognitive Sciences*, *8*(8), 347–355. <https://doi.org/10.1016/j.tics.2004.06.006>
- Honkanen, R., Rouhinen, S., Wang, S. H., Palva, J. M., & Palva, S. (2015). Gamma oscillations underlie the maintenance of feature-specific information and the contents of visual working memory. *Cerebral Cortex*, *25*(10), 3788–3801. <https://doi.org/10.1093/cercor/bhu263>

- Howard, M. W. (2003). Gamma oscillations correlate with working memory load in humans. *Cerebral Cortex*, *13*(12), 1369–1374. <https://doi.org/10.1093/cercor/bhg084>
- Humphreys, G. W. (2016). Feature confirmation in object perception: Feature integration theory 26 years on from the Treisman Bartlett lecture. *Quarterly Journal of Experimental Psychology*, *69*(10), 1910–1940. <https://doi.org/10.1080/17470218.2014.988736>
- Jensen, O., Kaiser, J., & Lachaux, J.-P. (2007). Human gamma-frequency oscillations associated with attention and memory. *Trends in Neurosciences*, *30*(7), 317–324. <https://doi.org/10.1016/j.tins.2007.05.001>
- Jensen, O., & Mazaheri, A. (2010). Shaping functional architecture by oscillatory alpha activity: Gating by inhibition. *Frontiers in Human Neuroscience*, *4*, 1–8. <https://doi.org/10.3389/fnhum.2010.00186>
- Kalfaoğlu, Ç., Stafford, T., & Milne, E. (2018). Frontal theta band oscillations predict error correction and posterror slowing in typing. *Journal of Experimental Psychology: Human Perception and Performance*, *44*(1), 69–88. <https://doi.org/10.1037/xhp0000417>
- Keil, A., & Müller, M. M. (2010). Feature selection in the human brain: Electrophysiological correlates of sensory enhancement and feature integration. *Brain Research*, *1313*, 172–184. <https://doi.org/10.1016/j.brainres.2009.12.006>
- Kelly, S. P., Lalor, E. C., Reilly, R. B., & Foxe, J. J. (2006). Increases in alpha oscillatory power reflect an active retinotopic mechanism for distracter suppression during sustained visuospatial attention. *Journal of Neurophysiology*, *95*(6), 3844–3851. <https://doi.org/10.1152/jn.01234.2005>
- Klimesch, W. (2012). Alpha-band oscillations, attention, and controlled access to stored information. *Trends in Cognitive Sciences*, *16*(12), 606–617. <https://doi.org/10.1016/j.tics.2012.10.007>
- Klimesch, W., Sauseng, P., & Hanslmayr, S. (2007). EEG alpha oscillations: The inhibition–timing hypothesis. *Brain Research Reviews*, *53*(1), 63–88. <https://doi.org/10.1016/j.brainresrev.2006.06.003>
- Knyazev, G. G. (2007). Motivation, emotion, and their inhibitory control mirrored in brain oscillations. *Neuroscience and Biobehavioral Reviews*, *3*(31), 377–395. <https://doi.org/10.1016/j.neubiorev.2006.10.004>
- Kok, P., Mostert, P., & de Lange, F. P. (2017). Prior expectations induce prestimulus sensory templates. *Proceedings of the National Academy of Sciences*, *114*(39), 10473–10478. <https://doi.org/10.1073/pnas.1705652114>
- Kriegeskorte, N., Simmons, W. K., Bellgowan, P. S. F., & Baker, C. I. (2009). Circular analysis in systems neuroscience: The dangers of double dipping. *Nature Neuroscience*, *12*(5), 535–540. <https://doi.org/10.1038/nn.2303>
- Kuhn, G., & Rensink, R. A. (2016). The vanishing Ball illusion: A new perspective on the perception of dynamic events. *Cognition*, *148*, 64–70. <https://doi.org/10.1016/j.cognition.2015.12.003>
- Lange, J., Keil, J., Schnitzler, A., van Dijk, H., & Weisz, N. (2014). The role of alpha oscillations for illusory perception. *Behavioural Brain Research*, *271*, 294–301. <https://doi.org/10.1016/j.bbr.2014.06.015>
- Leonards, U., Sunaert, S., Van Hecke, P., & Orban, G. A. (2000). Attention mechanisms in visual search—An fMRI study. *Journal of Cognitive Neuroscience*, *12*(Supplement 2), 61–75. <https://doi.org/10.1162/089892900564073>
- Leske, S., & Dalal, S. S. (2019). Reducing power line noise in EEG and MEG data via spectrum interpolation. *NeuroImage*, *189*, 763–776. <https://doi.org/10.1016/j.neuroimage.2019.01.026>
- Limbach, K., & Corballis, P. M. (2016). Prestimulus alpha power influences response criterion in a detection task. *Psychophysiology*, *53*(8), 1154–1164. <https://doi.org/10.1111/psyp.12666>
- Lundqvist, M., Herman, P., & Lansner, A. (2011). Theta and gamma power increases and alpha/beta power decreases with memory load in an attractor network model. *Journal of Cognitive Neuroscience*, *23*(10), 3008–3020. [https://doi.org/10.1162/jocn\\_a\\_00029](https://doi.org/10.1162/jocn_a_00029)
- Luu, P., Tucker, D. M., & Makeig, S. (2004). Frontal midline theta and the error-related negativity: Neurophysiological mechanisms of action regulation. *Clinical Neurophysiology*, *115*(8), 1821–1835. <https://doi.org/10.1016/j.clinph.2004.03.031>
- Mack, A., Erol, M., Clarke, J., & Bert, J. (2016). No iconic memory without attention. *Consciousness and Cognition*, *40*, 1–8. <https://doi.org/10.1016/j.concog.2015.12.006>
- Mapelli, I., & Özkurt, T. E. (2019). Brain oscillatory correlates of visual short-term memory errors. *Frontiers in Human Neuroscience*, *13*, 33. <https://doi.org/10.3389/fnhum.2019.00033>
- Mathes, B., Khalaidovski, K., Schmiedt-Fehr, C., & Basar-Eroglu, C. (2014). Frontal theta activity is pronounced during illusory perception. *International Journal of Psychophysiology*, *94*(3), 445–454. <https://doi.org/10.1016/j.ijpsycho.2014.08.585>
- Mathewson, K. E., Gratton, G., Fabiani, M., Beck, D. M., & Ro, T. (2009). To see or not to see: Prestimulus phase predicts visual awareness. *Journal of Neuroscience*, *29*(9), 2725–2732. <https://doi.org/10.1523/JNEUROSCI.3963-08.2009>
- Mayer, A., Schwiedrzik, C. M., Wibrall, M., Singer, W., & Melloni, L. (2016). Expecting to see a letter: Alpha oscillations as carriers of top-down sensory predictions. *Cerebral Cortex*, *26*(7), 3146–3160. <https://doi.org/10.1093/cercor/bhv146>
- Mazaheri, A., & Jensen, O. (2010). Rhythmic pulsing: Linking ongoing brain activity with evoked responses. *Frontiers in Human Neuroscience*, *4*, 177. <https://doi.org/10.3389/fnhum.2010.00177>
- Mazaheri, A., Nieuwenhuis, I. L. C., van Dijk, H., & Jensen, O. (2009). Prestimulus alpha and mu activity predicts failure to inhibit motor responses. *Human Brain Mapping*, *30*(6), 1791–1800. <https://doi.org/10.1002/hbm.20763>
- Mi, Y., Katkov, M., & Tsodyks, M. (2017). Synaptic correlates of working memory capacity. *Neuron*, *93*(2), 323–330. <https://doi.org/10.1016/j.neuron.2016.12.004>
- Michelmann, S., Bowman, H., & Hanslmayr, S. (2016). The temporal signature of memories: Identification of a general mechanism for dynamic memory replay in humans. *PLoS Biology*, *14*(8), e1002528. <https://doi.org/10.1371/journal.pbio.1002528>
- Miller, E. K., Lundqvist, M., & Bastos, A. M. (2018). Working memory 2.0. *Neuron*, *100*(2), 463–475. <https://doi.org/10.1016/j.neuron.2018.09.023>
- Min, B.-K., & Herrmann, C. S. (2007). Prestimulus EEG alpha activity reflects prestimulus top-down processing. *Neuroscience Letters*, *422*(2), 131–135. <https://doi.org/10.1016/j.neulet.2007.06.013>
- Min, B.-K., Park, J. Y., Kim, E. J., Kim, J. I., Kim, J.-J., & Park, H.-J. (2008). Prestimulus EEG alpha activity reflects temporal expectancy. *Neuroscience Letters*, *438*(3), 270–274. <https://doi.org/10.1016/j.neulet.2008.04.067>
- Montaser-Kouhsari, L., & Rajimehr, R. (2005). Subliminal attentional modulation in crowding condition. *Vision Research*, *45*(7), 839–844. <https://doi.org/10.1016/j.visres.2004.10.020>
- Morey, R. D. (2008). Confidence intervals from normalized data: A correction to Cousineau (2005). *Tutorials in Quantitative*



- Methods for Psychology*, 4(2), 61–64. <https://doi.org/10.20982/tqmp.04.2.p061>
- Morgan, H. M., Muthukumaraswamy, S. D., Hibbs, C. S., Shapiro, K. L., Bracewell, R. M., Singh, K. D., & Linden, D. E. J. (2011). Feature integration in visual working memory: Parietal gamma activity is related to cognitive coordination. *Journal of Neurophysiology*, 106(6), 3185–3194. <https://doi.org/10.1152/jn.00246.2011>
- Müller, N. G., Vellage, A.-K., Heinze, H.-J., & Zaehle, T. (2015). Entrainment of human alpha oscillations selectively enhances visual conjunction search. *PLoS One*, 10(11), e0143533. <https://doi.org/10.1371/journal.pone.0143533>
- Oostenveld, R., Fries, P., Maris, E., & Schoffelen, J.-M. (2011). FieldTrip: Open source software for advanced analysis of MEG, EEG, and invasive electrophysiological data. *Computational Intelligence and Neuroscience*, 2011, 1–9. <https://doi.org/10.1155/2011/156869>
- Pelli, D. G., Palomares, M., & Majaj, N. J. (2004). Crowding is unlike ordinary masking: Distinguishing feature integration from detection. *Journal of Vision*, 4(12), 1136–1169. <https://doi.org/10.1167/4.12.12>
- Pelli, D. G., & Tillman, K. A. (2008). The uncrowded window of object recognition. *Nature Neuroscience*, 11(10), 1129–1135. <https://doi.org/10.1038/nn.2187>
- Percival, D. B., & Walden, A. T. (1993). *Spectral analysis for physical applications*. Cambridge University Press. <https://cir.nii.ac.jp/crid/1130000795749350912>
- Pfurtscheller, G., Stancák, A., & Neuper, C. (1996). Event-related synchronization (ERS) in the alpha band—An electrophysiological correlate cortical idling: A review. *International Journal of Psychophysiology*, 24(1), 39–46. [https://doi.org/10.1016/S0167-8760\(96\)00066-9](https://doi.org/10.1016/S0167-8760(96)00066-9)
- Phillips, S., & Takeda, Y. (2009). Greater frontal-parietal synchrony at low gamma-band frequencies for inefficient than efficient visual search in human EEG. *International Journal of Psychophysiology*, 73(3), 350–354. <https://doi.org/10.1016/j.ijpsycho.2009.05.011>
- Phillips, S., Takeda, Y., & Singh, A. (2012). Visual feature integration indicated by pHase-locked frontal-parietal EEG signals. *PLoS One*, 7(3), e32502. <https://doi.org/10.1371/journal.pone.0032502>
- Popov, T., Jensen, O., & Schoffelen, J.-M. (2018). Dorsal and ventral cortices are coupled by cross-frequency interactions during working memory. *NeuroImage*, 178, 277–286. <https://doi.org/10.1016/j.neuroimage.2018.05.054>
- Prinzmetal, W., Henderson, D., & Ivry, R. (1995). Loosening the constraints on illusory conjunctions: Assessing the roles of exposure duration and attention. *Journal of Experimental Psychology: Human Perception and Performance*, 21(6), 1362–1375. <https://doi.org/10.1037/0096-1523.21.6.1362>
- Prinzmetal, W., Presti, D. E., & Posner, M. I. (1986). Does attention affect visual feature integration? *Journal of Experimental Psychology: Human Perception and Performance*, 12(3), 361–369. <https://doi.org/10.1037/0096-1523.12.3.361>
- Putman, P., van Peer, J., Maimari, I., & van der Werff, S. (2010). EEG theta/beta ratio in relation to fear-modulated response-inhibition, attentional control, and affective traits. *Biological Psychology*, 83(2), 73–78. <https://doi.org/10.1016/j.biopsycho.2009.10.008>
- Putman, P., Verkuil, B., Arias-Garcia, E., Pantazi, I., & van Schie, C. (2014). EEG theta/beta ratio as a potential biomarker for attentional control and resilience against deleterious effects of stress on attention. *Cognitive, Affective, & Behavioral Neuroscience*, 14(2), 782–791. <https://doi.org/10.3758/s13415-013-0238-7>
- Robertson, L. C. (2003). Binding, spatial attention and perceptual awareness. *Nature Reviews Neuroscience*, 4(2), 93–102. <https://doi.org/10.1038/nrn1030>
- Rodríguez-San Esteban, P., Chica, A., & Paz-Alonso, P. (2022). Functional characterization of correct and incorrect feature integration. *Cerebral Cortex*, 33, 1440–1451. <https://doi.org/10.1093/cercor/bhac147>
- Roehle, M. A., Kluger, D. S., Schroeder, S. C. Y., Schliephake, L. M., Boelte, J., Jacobsen, T., & Schubotz, R. I. (2021). Early alpha/beta oscillations reflect the formation of face-related expectations in the brain. *PLoS One*, 16(7), e0255116. <https://doi.org/10.1371/journal.pone.0255116>
- Rohenkohl, G., Bosman, C. A., & Fries, P. (2018). Gamma synchronization between V1 and V4 improves behavioral performance. *Neuron*, 100(4), 953–963.e3. <https://doi.org/10.1016/j.neuron.2018.09.019>
- Romei, V., Driver, J., Schyns, P. G., & Thut, G. (2011). Rhythmic TMS over parietal cortex links distinct brain frequencies to global versus local visual processing. *Current Biology*, 21(4), 334–337. <https://doi.org/10.1016/j.cub.2011.01.035>
- Rouhinen, S., Panula, J., Palva, J. M., & Palva, S. (2013). Load dependence of  $\beta$  and  $\gamma$  oscillations predicts individual capacity of visual attention. *Journal of Neuroscience*, 33(48), 19023–19033. <https://doi.org/10.1523/JNEUROSCI.1666-13.2013>
- Roux, F., & Uhlhaas, P. J. (2014). Working memory and neural oscillations: Alpha-gamma versus theta-gamma codes for distinct WM information? *Trends in Cognitive Sciences*, 18(1), 16–25. <https://doi.org/10.1016/j.tics.2013.10.010>
- Sammer, G., Blecker, C., Gebhardt, H., Bischoff, M., Stark, R., Morgen, K., & Vaitl, D. (2007). Relationship between regional hemodynamic activity and simultaneously recorded EEG-theta associated with mental arithmetic-induced workload. *Human Brain Mapping*, 28(8), 793–803. <https://doi.org/10.1002/hbm.20309>
- Sauseng, P., Griesmayr, B., Freunberger, R., & Klimesch, W. (2010). Control mechanisms in working memory: A possible function of EEG theta oscillations. *Neuroscience & Biobehavioral Reviews*, 34(7), 1015–1022. <https://doi.org/10.1016/j.neubiorev.2009.12.006>
- Sauseng, P., Klimesch, W., Stadler, W., Schabus, M., Doppelmayr, M., Hanslmayr, S., Gruber, W., & Birbaumer, N. (2006). A shift of visual spatial attention is selectively associated with human EEG alpha activity. *The European Journal of Neuroscience*, 22, 2917–2926. <https://doi.org/10.1111/j.1460-9568.2005.04482.x>
- Schneider, W., Eschman, A., & Zuccolotto, A. (2002). *E-Prime 2.0*. Psychology Software Tools, Inc.
- Schroeder, S. C. Y., Ball, F., & Busch, N. A. (2018). The role of alpha oscillations in distractor inhibition during memory retention. *European Journal of Neuroscience*, 48(7), 2516–2526. <https://doi.org/10.1111/ejn.13852>
- Schutter, D. J. L. G., & Van Honk, J. (2005). Electrophysiological ratio markers for the balance between reward and punishment. *Cognitive Brain Research*, 24(3), 685–690. <https://doi.org/10.1016/j.cogbrainres.2005.04.002>
- Senkowski, D., Schneider, T. R., Foxe, J. J., & Engel, A. K. (2008). Crossmodal binding through neural coherence: Implications

- for multisensory processing. *Trends in Neurosciences*, 31(8), 401–409. <https://doi.org/10.1016/j.tins.2008.05.002>
- Shafritz, K., Gore, J., & Marois, R. (2002). The role of the parietal cortex in visual feature binding. *Proceedings of the National Academy of Sciences of the United States of America*, 99, 10917–10922. <https://doi.org/10.1073/pnas.152694799>
- Shu, N., Gao, Z., Chen, X., & Liu, H. (2015). Computational model of primary visual cortex combining visual attention for action recognition. *PLoS One*, 10(7), e0130569. <https://doi.org/10.1371/journal.pone.0130569>
- Singer, W. (2013). Cortical dynamics revisited. *Trends in Cognitive Sciences*, 17(12), 616–626. <https://doi.org/10.1016/j.tics.2013.09.006>
- Snyder, S. M., & Hall, J. R. (2006). A meta-analysis of quantitative EEG power associated with attention-deficit hyperactivity disorder. *Journal of Clinical Neurophysiology*, 23(5), 441–456. <https://doi.org/10.1097/01.wnp.0000221363.12503.78>
- Son, D., Rover, M., De Blasio, F. M., Does, W., Barry, R. J., & Putman, P. (2019). Electroencephalography theta/beta ratio covaries with mind wandering and functional connectivity in the executive control network. *Annals of the New York Academy of Sciences*, 1452(1), 52–64. <https://doi.org/10.1111/nyas.14180>
- Soto, D., & Humphreys, G. W. (2009). Semantically induced distortions of visual awareness in a patient with Balint's syndrome. *Cognition*, 110, 237–241.
- Strüber, D., Basar-Eroglu, C., Hoff, E., & Stadler, M. (2000). Reversal-rate dependent differences in the EEG gamma-band during multistable visual perception. *International Journal of Psychophysiology*, 38(3), 243–252. [https://doi.org/10.1016/S0167-8760\(00\)00168-9](https://doi.org/10.1016/S0167-8760(00)00168-9)
- Sweeney-Reed, C. M., Riddell, P. M., Ellis, J. A., Freeman, J. E., & Nasuto, S. J. (2012). Neural correlates of true and false memory in mild cognitive impairment. *PLoS One*, 7(10), e48357. <https://doi.org/10.1371/journal.pone.0048357>
- Tallon-Baudry, C. (2009). The roles of gamma-band oscillatory synchrony in human visual cognition. *Frontiers in Bioscience (Landmark Edition)*, 14, 321–332. <https://doi.org/10.2741/3246>
- Tallon-Baudry, C., & Bertrand, O. (1999). Activity in humans and its role in object representation. *Trends in Cognitive Sciences*, 3(4), 12.
- Tallon-Baudry, C., Bertrand, O., Delpuech, C., & Pernier, J. (1996). Stimulus specificity of phase-locked and non-phase-locked 40 Hz visual responses in human. *The Journal of Neuroscience*, 16(13), 4240–4249. <https://doi.org/10.1523/JNEUROSCI.16-13-04240.1996>
- Thut, G. (2006). Band electroencephalographic activity over occipital cortex indexes visuospatial attention bias and predicts visual target detection. *Journal of Neuroscience*, 26(37), 9494–9502. <https://doi.org/10.1523/JNEUROSCI.0875-06.2006>
- Tootell, R. B. H., Hadjikhani, N. K., Vanduffel, W., Liu, A. K., Mendola, J. D., Sereno, M. I., & Dale, A. M. (1998). Functional analysis of primary visual cortex (V1) in humans. *Proceedings of the National Academy of Sciences*, 95(3), 811–817. <https://doi.org/10.1073/pnas.95.3.811>
- Treisman, A. (1996). The binding problem. *Current Opinion in Neurobiology*, 6(2), 171–178. [https://doi.org/10.1016/S0959-4388\(96\)80070-5](https://doi.org/10.1016/S0959-4388(96)80070-5)
- Treisman, A., & Schmidt, H. (1982). Illusory conjunctions in the perception of objects. *Cognitive Psychology*, 14(1), 107–141. [https://doi.org/10.1016/0010-0285\(82\)90006-8](https://doi.org/10.1016/0010-0285(82)90006-8)
- Treisman, A. M., & Gelade, G. (1980). A feature-integration theory of attention. *Cognitive Psychology*, 12, 97–136. [https://doi.org/10.1016/0010-0285\(80\)90005-5](https://doi.org/10.1016/0010-0285(80)90005-5)
- Trujillo, L. T., & Allen, J. J. B. (2007). Theta EEG dynamics of the error-related negativity. *Clinical Neurophysiology*, 118(3), 645–668. <https://doi.org/10.1016/j.clinph.2006.11.009>
- van den Berg, B., Appelbaum, L. G., Clark, K., Lorist, M. M., & Woldorff, M. G. (2016). Visual search performance is predicted by both prestimulus and poststimulus electrical brain activity. *Scientific Reports*, 6(1), 37718. <https://doi.org/10.1038/srep37718>
- van Dijk, H., Schoffelen, J.-M., Oostenveld, R., & Jensen, O. (2008). Prestimulus oscillatory activity in the alpha band predicts visual discrimination ability. *Journal of Neuroscience*, 28(8), 1816–1823. <https://doi.org/10.1523/JNEUROSCI.1853-07.2008>
- van Es, M. W. J., Marshall, T. R., Spaak, E., Jensen, O., & Schoffelen, J. (2022). Phasic modulation of visual representations during sustained attention. *European Journal of Neuroscience*, 55(11–12), 3191–3208. <https://doi.org/10.1111/ejn.15084>
- van Son, D., De Blasio, F. M., Fogarty, J. S., Angelidis, A., Barry, R. J., & Putman, P. (2019). Frontal EEG theta/beta ratio during mind wandering episodes. *Biological Psychology*, 140, 19–27. <https://doi.org/10.1016/j.biopsycho.2018.11.003>
- van Son, D., Schalbroeck, R., Angelidis, A., van der Wee, N. J. A., van der Does, W., & Putman, P. (2018). Acute effects of caffeine on threat-selective attention: Moderation by anxiety and EEG theta/beta ratio. *Biological Psychology*, 136, 100–110. <https://doi.org/10.1016/j.biopsycho.2018.05.006>
- Vandierendonck, A. (2017). A comparison of methods to combine speed and accuracy measures of performance: A rejoinder on the binning procedure. *Behavior Research Methods*, 49(2), 653–673. <https://doi.org/10.3758/s13428-016-0721-5>
- Veniero, D., Gross, J., Morand, S., Duecker, F., Sack, A. T., & Thut, G. (2021). Top-down control of visual cortex by the frontal eye fields through oscillatory realignment. *Nature Communications*, 12(1), 1757. <https://doi.org/10.1038/s41467-021-21979-7>
- Verguts, T., & Van Opstal, F. (2005). Dissociation of the distance effect and size effect in one-digit numbers. *Psychonomic Bulletin & Review*, 12(5), 925–930. <https://doi.org/10.3758/BF03196787>
- Vidal, J. R., Chaumon, M., O'Regan, J. K., & Tallon-Baudry, C. (2006). Visual grouping and the focusing of attention induce gamma-band oscillations at different frequencies in human magnetoencephalogram signals. *Journal of Cognitive Neuroscience*, 18(11), 1850–1862. <https://doi.org/10.1162/jocn.2006.18.11.1850>
- Whitney, D., & Levi, D. M. (2011). Visual crowding: A fundamental limit on conscious perception and object recognition. *Trends in Cognitive Sciences*, 15(4), 160–168. <https://doi.org/10.1016/j.tics.2011.02.005>
- Wutz, A., Melcher, D., & Samaha, J. (2018). Frequency modulation of neural oscillations according to visual task demands. *Proceedings of the National Academy of Sciences*, 115(6), 1346–1351. <https://doi.org/10.1073/pnas.1713318115>
- Yeshurun, Y., & Rashal, E. (2010). Precueing attention to the target location diminishes crowding and reduces the critical distance. *Journal of Vision*, 10(10), 16. <https://doi.org/10.1167/10.10.16>
- Zhang, Y., Zhang, Y., Cai, P., Luo, H., & Fang, F. (2019). The causal role of  $\alpha$ -oscillations in feature binding. *Proceedings of the National Academy of Sciences*, 116(34), 17023–17028. <https://doi.org/10.1073/pnas.1904160116>

## SUPPORTING INFORMATION

Additional supporting information can be found online in the Supporting Information section at the end of this article.

**Figure S1.** Averaged normalized TF representation (2–70 Hz and –600 to 1000 ms; time 0 ms represents the number onset). The colorbar indicates relative change to baseline (–500 to –200 ms). Data were averaged for all conditions, participants, and electrodes before bootstrapping.

**Figure S2.** On the left, topoplot showing the distribution of theta power (3–6 Hz) from 200 to 400 ms. The red asterisks represent the analyzed electrodes. The red circle represents a supplementary electrode analyzed for showing the additional peak (although with slightly lower values than parieto-occipital sites).

**Figure S3.** On the left, topoplot showing the distribution of alpha power (9–12 Hz) from 400 to 1000 ms. The red asterisks represent the analyzed electrodes. On the right, the averaged alpha power for all conditions in PO3/PO4 electrodes. The dashed line represents the peak of alpha power suppression at 675 ms.

**Figure S4.** On the left, topoplot showing the distribution of beta power (17–23 Hz) from 400 to 800 ms. The red asterisks represent the analyzed electrodes. The red circle represents a supplementary electrode analyzed for showing the additional peak (although with slightly higher values than C3/C4 electrodes). On the right, the averaged beta power for all conditions in C3/C4 electrodes (up) and CP1 (bottom). The dashed line represents the peak of beta power suppression. In C3/C4, power reduction peaked at 575 ms, while in CP1 it peaked at 900 ms.

**Figure S5.** On the left, topoplot showing the distribution of gamma power (40–60 Hz) from 400 to 600 ms. The red asterisks represent the analyzed electrodes. On the right, the averaged gamma power for all conditions in F7/F8 (up) and CPz (bottom) electrodes. The dashed line represents the maximum peak of gamma power for frontal and central electrodes at 450 ms.

**Figure S6.** The proportion of hits, illusions, errors, and unseen responses across blocks. In blocks 1–10, the target letter was always colored in green, blue, or yellow (expected blocks). In blocks 11–12, the target letter was colored in white in 50% of the trials (unexpected blocks). The asterisks represent significant differences in the proportion of each trial type between consecutive blocks (indicated by gray shading) ( $***p < .001$ ;  $**p < .005$ ;  $*p < .05$ ).

**Figure S7.** Mean RT to respond to the central task as a function of Central Task condition and Trial Type. This figure shows the main effects of Central Task and Trial Type. Asterisks represent significant effects ( $***p < .001$ ).

**Figure S8.** Mean ACC in the central task as a function of Central Task condition and Trial Type. This figure shows the main effects of Central Task and Trial Type. Asterisks represent significant effects ( $***p < .001$ ;  $*p < .05$ ).

**How to cite this article:** Cobos, M. I., Melcón, M., Rodríguez-San Esteban, P., Capilla, A., & Chica, A. B. (2023). The role of brain oscillations in feature integration. *Psychophysiology*, 00, e14467. <https://doi.org/10.1111/psyp.14467>